University of New Mexico
UNM Digital Repository

Electrical and Computer Engineering ETDs Engineering ETDs

6-26-2015

# IN SITU PLASMA REMOVAL OF SURFACE CONTAMINANTS FROM ION TRAP ELECTRODES

Raymond Haltli

Follow this and additional works at: https://digitalrepository.unm.edu/ece_etds

Recommended Citation
Haltli, Raymond. "IN SITU PLASMA REMOVAL OF SURFACE CONTAMINANTS FROM ION TRAP ELECTRODES." (2015). https://digitalrepository.unm.edu/ece_etds/111

This Thesis is brought to you for free and open access by the Engineering ETDs at UNM Digital Repository. It has been accepted for inclusion in Electrical and Computer Engineering ETDs by an authorized administrator of UNM Digital Repository. For more information, please contact disc@unm.edu.

Raymond A Haltli
*Candidate*

Electrical and Computer Engineering
*Department*

This thesis is approved, and it is acceptable in quality and form for publication:

*Approved by the Thesis Committee:*

Dr. Charles B. Fleddermann , Chairperson

Dr. Meeko Oishi

Dr. Mathew G. Blain

**_IN SITU_ PLASMA REMOVAL OF SURFACE CONTAMINANTS FROM ION TRAP ELECTRODES**

**by**

**RAYMOND A. HALTLI**

**B.S., ELECTRONICS ENGINEERING TECHNOLOGY**
**DEVRY UNIVERSITY, 2003**

THESIS

Submitted in Partial Fulfillment of the
Requirements for the Degree of

**Masters of Science**
**Electrical Engineering**

The University of New Mexico
Albuquerque, New Mexico

**May 2015**

# Acknowledgments

First I would like to thank my friend and mentor, Matthew Blain, at Sandia National Laboratories for all the help, patience, encouragement, expertise, enlightening conversation and ideas through this project. He has always been available and willing to help.

I would like to thank Michael Brumbach at Sandia Labs for his work, which made the success of this project possible. His wealth of experience and suggestions he shared were invaluable.

I would like to thank my advisor, Dr. Charles Fleddermann, for his advice and support and for making this experience possible.

I would like to thank Peter Maunz for always being available for discussion and suggestions regarding how to move the work forward. Also, Peter was the PI on the IARPA MQCO Project, which funded this work. I would like to thank Boyan Tabakov, UNM and SNL for his feedback and informative discussions and for his experimental work making heating rate measurements, which gives meaning to the results in this project.

I would also like to thank others at Sandia, including Todd Bauer for helping me. Also, I appreciate Craig Clark for his enthusiasm for this endeavor and his motivation in getting the project started. Thanks also due to Ed Barnat for his expertise.

My thanks also go to the whole IARPA MQCO ion trapping team at Sandia for their scientific and engineering feedback and encouragement.

I would like to thank my manager, Mike Descour, for his support and encouragement. He helped me get accepted to the University Part-Time (UPT) program at SNL, which also made this work possible. I would like to thank the UPT program, for making available the opportunity to pursue higher education while working at Sandia.

I would like to thank Dr. Meeko Oishi for her encouragement in my education.

Not the least of all, I want to thank my wife, Jenny Haltli, who has always believed in me and supported me, and without whom I would not have been able to accomplish this project. She gave up many nights and weekends to allow me to focus. Jenny also helped immensely on grammatical editing and preparing the final draft of this thesis. I would like to thank all my family and friends for their encouragement and support.

Finally, I would like to thank my employer and the projects that funded this research. This work is part of the Multi-Qubit Coherent Operations (MQCO) program supported by the Intelligence Advanced Research Projects Activity (IARPA).

Sandia National Laboratories is a multi-program laboratory managed and operated by Sandia Corporation, a wholly owned subsidiary of Lockheed Martin Corporation, for the US Department of Energy's National Nuclear Security Administration under contract DE-AC04-94AL85000.

*IN SITU* **PLASMA REMOVAL OF SURFACE CONTAMINANTS FROM ION TRAP ELECTRODES**

**by**

**Raymond Haltli**

**Bachelors BS Electronics Engineering DeVry University, 2003**

**MS Electrical Engineering University of New Mexico**

## Abstract

In this thesis, the construction and implementation of an *in situ* plasma discharge designed to remove surface contaminants from electrodes in an ion trapping experimental system is presented with results. In recent years, many advances have been made in using ion traps for quantum information processing. All of the criteria defined by DiVincenzo for using ion traps for implementing a quantum computer have been individually demonstrated, and in particular surface traps provide a scalable platform for ions. In order to be used for quantum algorithms, trapped ions need to be cooled to their motional (quantum mechanical) ground state. One of the hurdles in integrating surface ion traps for a quantum computer is minimizing electric field noise, which causes the ion to heat out of its motional ground state and which increases with smaller ion-to-electrode distances realized with surface traps. Surface contamination of trap electrodes is speculated to be the primary source of electric field noise.

The main goal achieved by this work was to implement an *in situ* surface cleaning solution for surface electrode ion traps, which would not modify the ion trap electrode surface metal. Care was taken in applying the RF power in order to localize a plasma near the trap electrodes. A method for characterizing the energy of the plasma ions arriving at the ion trap surface is presented and results for plasma ion energies are shown. Finally, a method for quantifying the effectiveness of plasma cleaning of trap electrodes, using the surface analysis technique of X-ray photoelectron spectroscopy for measuring the amount and kind of surface contaminants, is described. A significant advantage of the trap electrode surface cleaning method presented here is the minimal changes necessary for implementation on a working ion trap experimental system.

# Table of Contents

**List of Figures** ..... **ix**

**List of Tables** ..... **xii**

**Chapter 1 Introduction** ..... **1**

Overview of Ion Trapping ..... 1

Heating Sources ..... 4

Heating Rate Reduction Techniques ..... 6

**Chapter 2 Experimental Setup** ..... **9**

Trap Fabrication ..... 9

Vacuum Chamber Description ..... 11

Vacuum Quality and Gas Introduction ..... 13

Plasma and Plasma Discharge Configurations ..... 14

Capacitively Coupled Plasma ..... 16

Inductively Coupled Plasma ..... 19

Retarding Field Ion Energy Analysis ..... 22

X-ray Photoelectron Spectroscopy (XPS) ..... 26

**Chapter 3 Experimental Results** ..... **29**

Vacuum Pressure Test ..... 29

Capacitively Coupled Plasma ..... 31

Inductively Coupled Plasma ..... 35

Ion Energy Measurements ..... 37

Heating Rate Measurements ..... 51

**Chapter 4 Summary and Conclusions** ..... **56**

**References ........................................................................................................ 59**

# List of Figures

Figure 1-1 Diagram of Linear Paul and Surface traps ........ 3

Figure 1-2 Diagram of quantum charge-coupled device (QCCD)........ 3

Figure 1-3 Realizations of surface electrode ion traps........ 4

Figure 2-1 Ion trap chip packaged in a CPGA........ 10

Figure 2-2 Cross-sectional SEM of the ion trap ........ 11

Figure 2-3 Ion trapping chamber with pumping manifold........ 12

Figure 2-4 Bottom flange with ion trap in the socket ........ 13

Figure 2-5 Schematic of plasma power supply........ 15

Figure 2-6 Concept for capacitively coupled plasma ........ 17

Figure 2-7 Screens and ion trap chips........ 17

Figure 2-8 Ceramic PGA package with seal ring labeled........ 17

Figure 2-9 Prepared trap chip with SMA attached ........ 18

Figure 2-10 Virgin CPGA package, shadow mask for gold coating, gold ground ring evaporated onto CPGA ........ 18

Figure 2-11 Diagram of induced E-field in the plasma ........ 19

Figure 2-12 Configuration for inductively coupled plasma........ 21

Figure 2-13 Ion trapping chamber shown with RF plasma coil on re-entrant viewport ........ 22

Figure 2-14 Packaged retarding field energy analyzer ........ 23

Figure 2-15 Cross-sectional images of retarding field energy analyzer ........ 24

Figure 2-16 Process flow for retarding field energy analyzer ........ 24

Figure 2-17 Repeller scan ........ 25

Figure 2-18 Collector scan and ion energy distribution........................................... 26

Figure 3-1 Drawing of simplified chamber for UHP gas introduction test ................ 30

Figure 3-2 Diffuse plasma in test chamber, low millitorr pressure about 20 W......... 32

Figure 3-3 Localized capacitive plasma not covering the center of the ion trap ........ 33

Figure 3-4 Sputtered gold from high ion energies .................................................... 34

Figure 3-5 Capacitively coupled plasma discharge configurations ............................ 35

Figure 3-6 Inductively coupled plasma setup ........................................................... 36

Figure 3-7 Image of localized plasma directly above the ion trap surface ................. 37

Figure 3-8 Initiation power vs. pressure curve .......................................................... 37

Figure 3-9 Ion energy distribution, Retarding Field Analyzer Repeller Voltage ....... 38

Figure 3-10 Ion energies for various pressures.......................................................... 39

Figure 3-11 Sputter yields for low energy argon ions ................................................ 40

Figure 3-12 Ring shaped ion trap divided by gold and aluminum ............................. 41

Figure 3-13 Pre-plasma XPS scan on the gold side.................................................... 42

Figure 3-14 Pre-plasma XPS scans on the aluminum side ......................................... 42

Figure 3-15 Plasma test chamber attached to XPS analysis system ........................... 45

Figure 3-16 Half of the surface electrode ring trap coated with gold.......................... 46

Figure 3-17 XPS results in test chamber with carbon tape fixing trap chip, C 1s spectra, 5 minutes argon plasma exposure, 4 W, 72 MHz, 250 mTorr ........ 46

Figure 3-18 XPS spectrum of carbon and oxygen peaks on gold and aluminum surfaces pre- and post-plasma exposure, 72 MHz, 4 W, 300 s............................ 47

Figure 3-19 XPS spectrum on gold and aluminum pre-plasma and post-plasma showing an increasing carbon peak even while in XPS vacuum chamber

including +1.5hrs, +8hrs, +14hrs ........ 49

Figure 3-20 Timed plamsa exposure at 250 mTorr, 72 MHz, 4 W ........ 50

Figure 3-21 Timed plamsa exposure at 500 mTorr, 72 MHz, 4 W ........ 51

Figure 3-22 Timed plamsa exposure at 75 mTorr, 72 MHz, 4 W ........ 51

Figure 3-23 HOA2 ion trap chip ........ 52

Figure 3-24 Ion heating rate measurements pre- and post-plasma showing no measurable change ........ 53

# List of Tables

Table 2-1 Inductive plasma parameters vs capacitive ............................................... 20

Table 3-1 Pre-plasma treatment concentrations by atomic percent taken from XPS scans on the Gold side of each sample................................................................ 43

Table 3-2 Plasma treatment conditions, for all conditions the frequency was 72MHz the forward power was 4 watts and the pressure was 250 mTorr............ 43

Table 3-3 Post-plasma treatment concentrations by atomic percent taken from XPS scans on the Gold side of each sample................................................................ 44

Table 3-4 Summary of plasma results by XPS atomic percent carbon....................... 48

# Chapter 1

# Introduction

Trapped ions are studied and manipulated in many areas of physics, including in research to develop a quantum information processor. With precise control of trapped ions, collective motion multi-qubit logic gates can be formed for this purpose. One of the principal difficulties in performing quantum operations using ions is the rate at which the ions heat from their motional ground state causing errors in the qubits. There are diverse sources of ion heating; the source explored here is surface contaminants. In this work an *in situ* plasma system designed to remove surface contaminants in an ion trap system is presented with results.

## Overview of Ion Trapping

An ion is an electrically charged atom or molecule created by adding or removing an electron. Ions can be trapped in an electromagnetic field and used for a number of scientific applications including mass spectrometry, atomic clocks, basic atomic physics research, and controlling quantum states. For the work described in this paper, atomic calcium is the ion, which is trapped and controlled.

The end goal of trapping, cooling, and controlling ions in this context is to create a system of qubits or quantum gates that can execute quantum algorithms. There are some algorithms, like Shor's algorithm, which have been proven to factor numbers faster than any known method on a classical computer[1]. An in-depth review of quantum computation can be found in the book by Nielsen and Chuang [2].

A quantum processor is attractive because, in theory, it would be able to perform complex operations that modern classical computers cannot. These complex operations are made possible because of the principle of quantum superposition which allows large numbers of computations to be performed simultaneously [3].

The Paul trap and the Penning trap are the two most common types of ion traps. In a Paul trap, the ion is confined solely with oscillating electric fields. In contrast, the Penning trap uses a strong homogeneous magnetic field and a weak quadrupolar electrostatic potential. The work presented here is performed using Paul traps. The three-dimensional Paul trap consists of four rods and two end caps (Figure 1-1). An RF electrical signal is applied to two of the rods opposite each other and the other two rods are held at ground. A DC potential is applied to the end caps. The time-averaged potential of this configuration creates a pseudo-potential null, a time averaged potential of which is where the ion is confined. Trapping results from a restoring force that confines the ion. This can be envisioned as a marble placed on a saddle. If the saddle is left static, the marble will simply roll from any point down until it falls. But if the saddle is rotated at the correct frequency, the marble is not allowed to fall down the sides, because it is continuously pushed back to the center by the high points as they rotate past the marble. Similarly, the frequency and voltage of the RF fields in an ion trap are defined to trap the ion in the time averaged null.

For quantum information processing to be realized, multiple ions and many trapping wells are needed. The wells are connected with shuttling regions and junction regions for transporting ions. A three dimensional (3D) realization would be challenging, if not impossible, to build with enough trapping regions for quantum information

processing. Therefore, to realize a quantum processor with enough shuttle and junction regions, the 3D trap has been flattened, and is now fabricated using a combination of semiconductor manufacturing processes of integrated circuits (IC's) and micro-electromechanical systems (MEMS). This surface trap arrangement is described by Chiaverini, *et al*. and is pictured below (Figure 1-1) [4]. The most promising arrangement of quantum charge-coupled device was first proposed by Kielpinski, *et al*. which allows for different regions for shuttling, computation and storage [5] as shown in Figure 1-2.

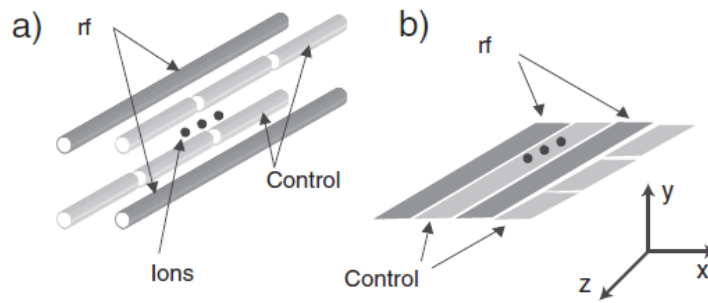


Figure 1-1: (a) Linear Paul trap; (b) Surface trap, electrodes flattened in a plane [4]

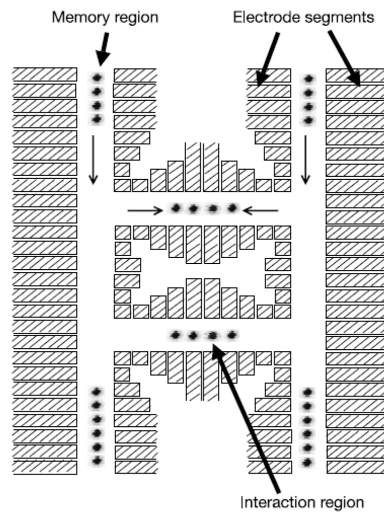


Figure 1-2: Diagram of quantum charge-coupled device (QCCD) first proposed by Kielpinski *et al.* [5]

Among the most advanced surface traps that have been constructed are those described by Moehring [6]. A trap with many shuttle and junction regions can be fabricated by using a multilevel metal process to route electrical leads in a buried metal layer shielded from the RF electrode. In addition, because of the unique fabrication technology of traps constructed at Sandia National Laboratories, there are no exposed dielectrics in line-of-sight of the trapped ion. This is an important feature that prevents shorting of electrodes when they are exposed to sputtered or evaporated metals. Some of these surface trap realizations are shown in Figure 1-3.

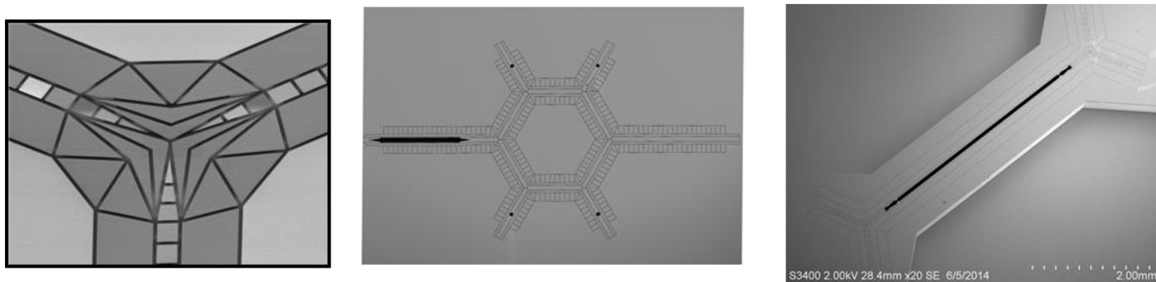


Figure 1-3: Realizations of surface electrode ion traps at Sandia National Laboratories

## **Heating Sources**

For quantum information processing, a system needs to bring together trapped ions to form qubits. Ions need to be cooled down to the motional ground state in order to be useful. Qubits are then used to perform computational operations. If decoherence occurs before the computational operation, then an error in the system occurs. One of the hurdles in building a quantum processor is overcoming electric field noise in the system, which can cause decoherence errors. Heating of the trapped ion from its motional ground

state is one of the consequences of electric field noise and one cause of decoherence in the system, that limits the fidelity of gate operations. Heating is an increase in the ions' number of motional quanta, and if the ion heats up enough, it can escape the trap. For an extensive summary of heating rate measurements in ion traps see the review by Brownnutt *et al.* [7].

The sources of heating are not well understood. According to Turchette, *et al.* [8] some of the possible mechanisms are Johnson noise, fluctuating patch potentials, ambient electric fields, fields generated by fluctuating currents, and collisions with background atoms. Turchette proposed a model of fluctuating patch-potential noise and proposed that a cleaning method should be used to solve this problem.

Daniilidis, *et al*. [9] performed heating rate experiments showing surface contaminants contribute to the heating rate. They followed the analysis of Volokitin and Persson [10] and showed that surface adsorbates could be one source of anomalous heating. In their experiments, they measured heating rates in a surface electrode ion trap. They observed that over time the heating rate increased more in the ion loading zone than in other regions of the trap. This result suggests that surface contamination associated with ion loading is an important source of anomalous heating and may require less than a monolayer of contamination. Daniilidis, *et al*. proposed that specific care would need to be taken to target and remove adsorbates from metal surfaces [9].

Surface adsorbates are not the only form of contamination on trap electrodes. It is known that carbon species readily adsorb on metal surfaces [11]. In the work presented here carbon and oxygen on gold and aluminum trap electrode surfaces are quantitatively measured using XPS surface analysis and removed using *in situ* plasma.

## **Heating Rate Reduction Techniques**

Surface properties impact the heating rate of an ion in a trap [12]. Several methods have been explored for lowering the effect of the surrounding environment on the heating rate of trapped ions including cryogenic cooling [13], laser cleaning [14], and argon ion beam sputtering of trap electrode surfaces [15].

Cryogenic cooling of trap electrodes is one method for reducing heating rates. This method reduces both Johnson noise and the effects of anomalous heating. Adding cryogenic cooling greatly increases the complexity of the ion trapping experimental chamber and does not remove the adsorbates from the surface but suppresses their effects. Antohi, *et al*. [13] showed heating rate reduction of seven to eight orders of magnitude by cooling the ion trap electrodes to 6K. Because of the complexities added by cryogenic cooling, a method of reducing ion heating rates when operating traps at room temperature is still desirable. Cleaning the adsorbates from the surface may accomplish this.

Laser cleaning of the surface performed at Oxford was the first attempt at removing the source of anomalous heating due to surface adsorbates. Although laser ablation caused some damage to the electrodes of the ion trap, room temperature reduction of electric field noise by about 50% was observed [14]. The laser beam has a small spot size and therefore would require a raster pattern across the device which may prove to be a prohibitive factor in effective surface cleaning.

Hite, *et al*. [15] at NIST used a beam of argon ions to remove surface adsorbates and reported a reduction of two orders of magnitude in the heating rate at room

temperature. Ion energies of 2 keV and 500 eV were tried with varying results. These energies are well above the sputter threshold for gold and are certainly modifying the metal surface [16]. Furthermore this method is also localized and like laser cleaning requires a raster pattern across the device which may not provide the desired result. If the sputter beam comes from only one angle, the sputtered electrode material can re-deposit behind features on the trap surface, this is known as shadowing. Although surface modifications appear to be important in reducing heating rates, sputtering the electrode surface needs to be done with great care to avoid shorting electrodes with the re-deposited metal.

The work presented here focusses on argon plasma cleaning as a method of removing surface contaminants from ion trap electrodes without modification of the underlying electrode material. The emphasis is on the design, implementation, and investigation of an argon plasma that is generated *in situ* and localized above the trap surface and on measuring the effectiveness of removing surface contaminants. As it is important to uniformly clean the surface of the trap and eliminate the need to raster across the surface, it is suggested that plasma may be the preferred method for accomplishing this. It is important that the plasma is not formed in other locations of the trapping experimental chamber which could allow trap surface contamination from other components. The ion energies from the plasma impinging on the surface of the chip are demonstrated to be above desorption energies of the surface contaminant and below the (appreciable) sputter threshold for the gold-gold or other metal surface bonds. This method removes surface adsorbates while not appreciably changing the metal electrode surface. By minimizing or eliminating gold atoms sputtered from the surface during

plasma cleaning the danger of shorting adjacent control electrodes with re-deposited gold is minimized. The plasma system designed here is used to clean ion traps *in situ*.

# Chapter 2

# Experimental Setup

In this chapter, the approach for implementing plasma cleaning in a surface ion trap experimental chamber is explained. There are many different varieties of ion traps from hand-assembled macroscopic traps [17] to monolithically integrated micro-fabricated traps. Ion traps operate at ultra-high vacuum (UHV) pressures of $10^{-11}$ Torr to minimize collisions between background gasses and trapped ions. For *in situ* plasma cleaning of an ion trap, the pressure in the vacuum chamber must be increased to the $10^{-3}$ to 1 Torr range. Additionally, for plasma cleaning, care is taken in applying the RF power in order to localize plasma near the trap electrodes. A method for characterizing the energy of the plasma ions arriving at the ion trap surface is presented and results for plasma ion energies are shown. Finally, as a method of quantifying the effectiveness of plasma cleaning of trap electrodes, the surface analysis technique of X-ray photoelectron spectroscopy (XPS) for measuring the amount and kind of surface contaminants is described.

Two vacuum chambers were used to perform experiments. One chamber was dedicated primarily to plasma characterization. The second chamber was dedicated to ion trapping for measuring heating rates and exposing a working ion trap to *in situ* plasma cleaning processes.

## Trap Fabrication

Surface ion trap fabrication is, by nature, a clean and well controlled process that uses complimentary metal-oxide-semiconductor (CMOS) and/or microelectromechanical

systems (MEMS) fabrication techniques. The surface ion traps used here consist of electrodes defined in Al-0.5%Cu metal and $SiO_2$ inter-metal dielectric to separate the electrode level (top metal) from the underlying routing layers as described in [6] [18]. Chemical mechanical planarization (CMP) is used to render a planar surface electrode trap. After electrode fabrication and release (removal of dielectric materials between electrodes), arbitrarily chosen metals can be evaporated onto the surface of the traps, as the removal of adjacent dielectric materials prevents shorting by the subsequently evaporated metal. The ion trap chip is mounted in a ceramic pin grid array package (CPGA) (Figure 2-1).

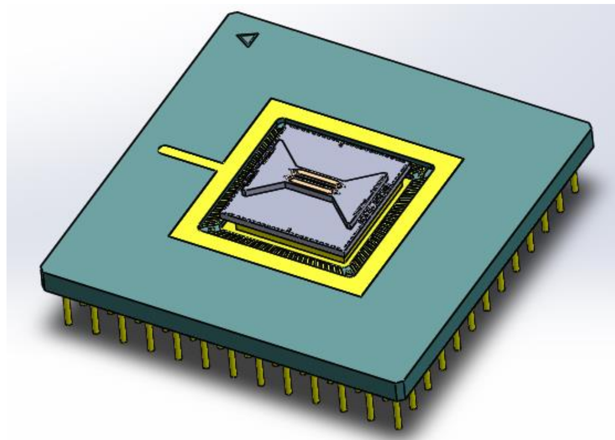

Figure 2-1: Ion trap chip packaged in a ceramic pin grid array (CPGA) package.

The electrode metal overhangs the underlying oxide supports as seen in Figure 2-2. Examples of various metals that have been used as ion trap electrodes are aluminum, gold, silver, and niobium. Aluminum is commonly used in CMOS processing and therefore an obvious choice for surface electrode ion traps. One downside to aluminum is the native oxide, $Al_2O_3$, which is formed on its surface. Since oxide is a poor electrical

conductor it can support unpinned charges thereby affecting the electrical field at the position of the ion in an ion trapping experiment. As these fields are undefined and can fluctuate in time they can serve as a source of electric field noise and lead to higher ion heating rates. Gold is a noble metal, and because it does not form a native oxide, it is commonly used for surface traps. However carbon species can contaminate the gold and support charge, which also represents an unpinned potential. Niobium is desirable because at temperatures below 9.2 K it is a super conductor [19]. The interaction of unpinned potentials with the ion needs to be eliminated and/or minimized. To this end, plasma cleaning is used to remove surface adsorbates.

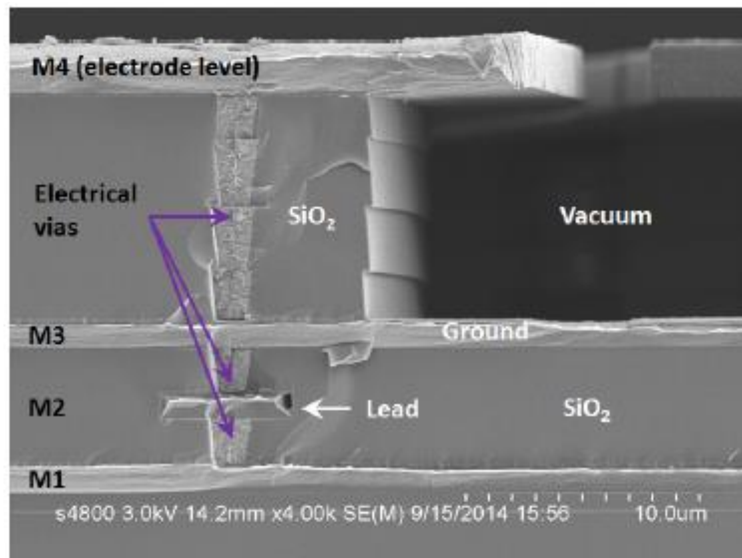


Figure 2-2: Cross-sectional SEM of the trap, showing the four metal levels, interconnects, and insulators.

## Vacuum Chamber Description

A representative ion trap chamber, such as that used at Sandia National Laboratories (SNL), is built using a Kimball Physics spherical octagon with ConFlat (CF) flanges (Figure 2-3). The trapping chamber is equipped with viewports for laser access

and imaging of the ion and a feed-through for radio frequency (RF) power delivery to the trap. One port of the octagon is connected to a pumping manifold that conducts gas molecules to an ion gauge, an ion pump, a titanium sublimation pump and a bakeable valve that temporarily connects a turbomolecular pump (TMP) for preparing the ultra-high vacuum (UHV) environment.

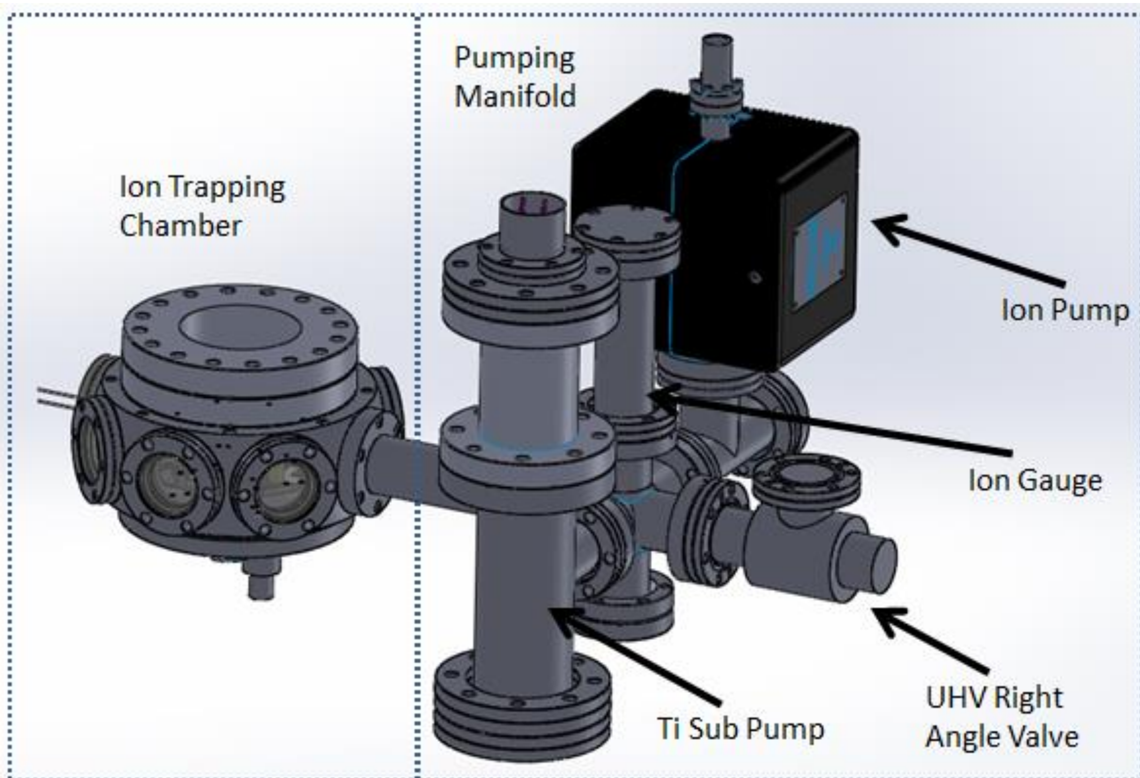


Figure 2-3: Ion trapping chamber with pumping manifold.

The bottom flange is equipped with an electrical feedthrough for the control electrodes on the ion trap that are used for transporting the ion and a feedthrough for the atomic source (Figure 2-4). The atomic source, an oven which is filled with calcium, for example, is heated until neutral atoms evaporate and pass through the trapping region

where they are photo-ionized and trapped. The top flange is a re-entrant view port where a lens and camera are mounted to collect photons emitted by the trapped ion.

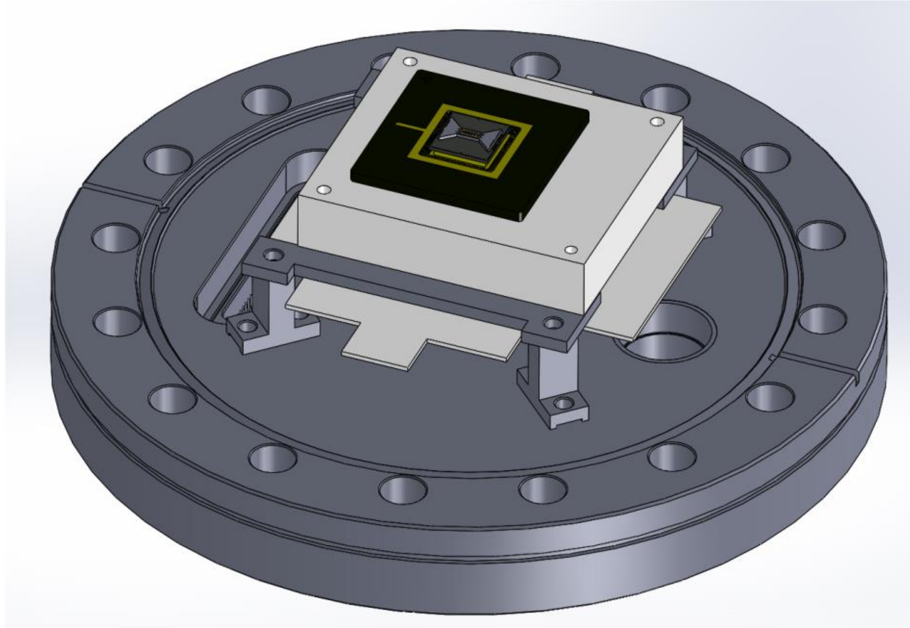

Figure 2-4: Bottom flange with ion trap in the socket.

Inside the chamber, there is a socket for delivering RF and DC control signals to the ion trap. A grounded screen between the re-entrant viewport window and the ion trap shields the ion trap from stray/unpinned potentials on the quartz window.

## Vacuum Quality and Gas Introduction

It is important for an ion trapping system to work at the lowest pressure possible. If the pressure in the system is too high, the background atoms in the chamber will have a higher frequency of colliding with the trapped ion and knocking it out of the trap. Trapped ion lifetimes need to be long enough to perform quantum operations.

Ion trapping chambers in the lab at SNL are prepared and maintained at a pressure in the range of $10^{-11}$ Torr. All chamber components are carefully chosen to be ultra-high vacuum (UHV) compatible. The chamber and all of its components are thoroughly cleaned and assembled in a cleanrooom environment. To reach UHV, it is necessary to bake the vacuum chamber for about one week at 200 ºC while a TMP and an ion pump are evacuating the system. One purpose of the increased temperature is to desorb water from internal surfaces. This bake is also a possible source for surface adsorbates on the ion trap chip, which is an undesirable consequence. When the chamber is returned to room temperature, a titanium sublimation pump is used to further reduce the vacuum pressure.

In order to perform plasma cleaning, argon gas is introduced into the chamber. A major preliminary consideration for the work here is that the chamber base pressure returns back to the $10^{-11}$ Torr range after the chamber has been raised to the millitorr range necessary for plasma ignition and cleaning. Ultra-high purity (99.9999%) argon is used and a clean gas manifold is attached to the vacuum chamber. It was shown in a test chamber that the chamber could be returned to UHV conditions without baking.

## **Plasma and Plasma Discharge Configurations**

Plasma is considered the fourth state of matter [20]. Plasma is formed in a gas when electrons are liberated from atoms or molecules by an energy source which can be electrical, thermal, or optical. If there is insufficient power, the electrons and ions will recombine. Langmuir was the first to apply the word “plasma” to ionized gas in 1929

[21]. Due to the approximately equal number of ions and electrons in the plasma, it is typically defined as quasineutral.

The plasma is charged positively with respect to any large electrode or wall surface. The region between the wall and the plasma is called the sheath; it is a visibly dark, positive space charge region. Plasma electrons have small mass and high temperature compared with plasma ions and, therefore, quickly move to any close surface. This process creates the plasma sheath as well as sets up a positive plasma potential with respect to the nearby surfaces.

There are many configuration options available for initiating a plasma discharge. The configurations explored in this work were capacitively coupled plasma and inductively coupled plasma both driven by a radio frequency (RF). The RF power was supplied using a signal generator which feeds an amplifier connected to a tunable impedance matching network Figure 2-5.

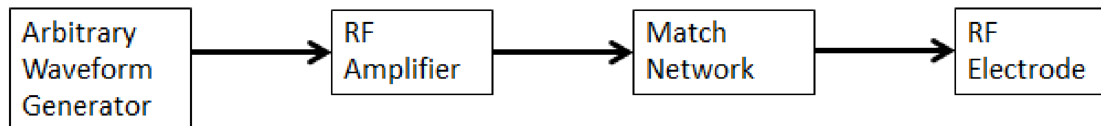


Figure 2-5: Schematic of plasma power supply

The ion trap experimental chamber needs only slight modifications to implement a plasma discharge capability. An additional bakeable valve is added to the bottom flange for introduction of the ultra-high purity gas. Other minor changes detailed below are specific to the type of discharge being implemented. A test chamber was specifically built

for the purpose of plasma testing and characterization. The main difference between the trapping chamber and the test chamber is that, for the test chamber, the pumping manifold, containing the ion pump, the ion gauge, and the titanium sublimation pump, was omitted.

## Capacitively Coupled Plasma

To implement a capacitively coupled plasma (CCP), an RF electrode as well as a ground is necessary. When the electric field is large enough, the gas breaks down and a plasma is formed. Plasma potentials in capacitive discharges can be high, resulting in ion acceleration energies across the sheath greater than 200 eV [22]. Capacitive plasmas are low density plasmas. One of the consequences of the plasma being low density is the low ion flux across the sheath.  The ion energy and flux in a CCP cannot be varied independently, and depend on discharge power, pressure and the ratio of RF to ground electrode areas [22].

One of the design concepts in this work is to minimize changes to the existing setup used in ion trapping vacuum chambers. The concept as shown in Figure 2-6 is to generate a localized plasma directly above the ion trap surface. With the plasma confined between the screen and the trap chip, ion bombardment of the re-entrant window is minimized and, therefore, potential damage would be minimized as well. In this setup, RF power can be delivered to either the screen (Figure 2-7) or the metal ring on the ceramic package called the seal ring (Figure 2-8). Both options were explored.

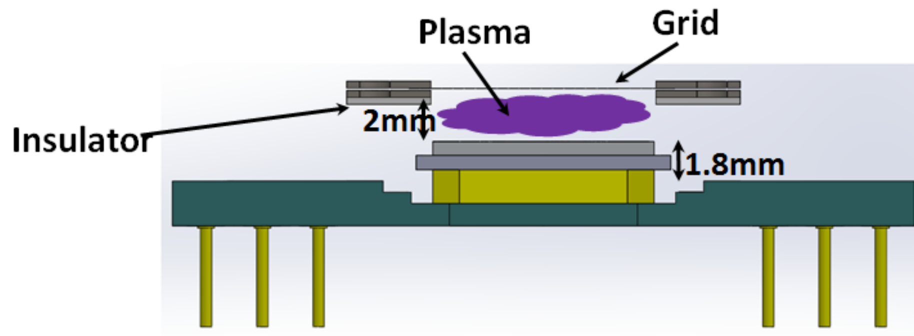


Figure 2-6: Concept for capacitively coupled plasma

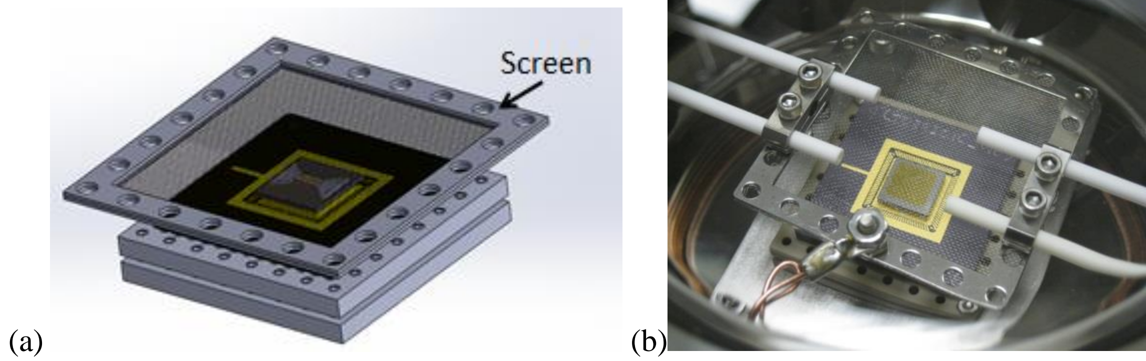


Figure 2-7: (a)Screen and ion trap chip (b) Actual screen and ion trap chip

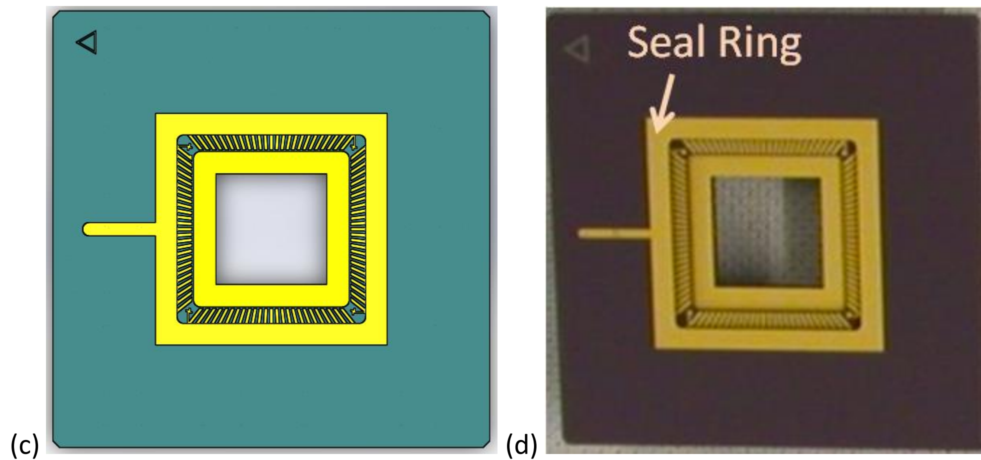


Figure 2-8: (a) Ceramic PGA package (b) Picture of package with seal ring labeled

For both implementations described an additional RF feedthrough was added to the vacuum chamber to deliver RF power for the plasma. In the first application, RF power was applied to the screen as shown in Figure 2-7(b) via a bare copper wire. The second configuration applied RF power to the seal ring of the package. To achieve this, an SMA connector was soldered to the package (Figure 2-9). An additional ring of gold was deposited for the grounding contacts of the connector (Figure 2-10). Because of limitations discovered while implementing capacitive discharges, inductive discharges were explored.

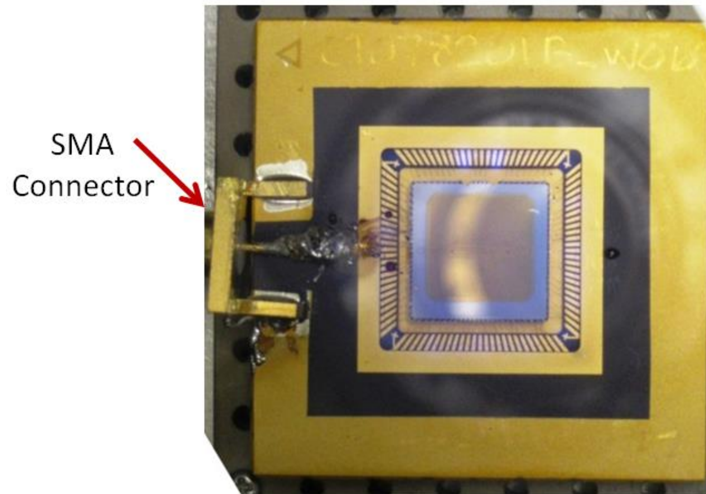


Figure 2-9: Prepared trap chip with SMA attached

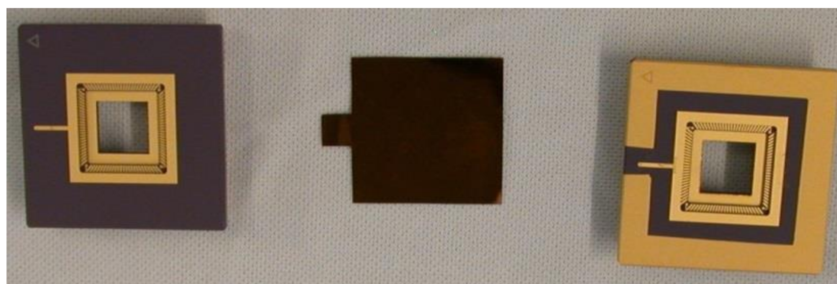

Figure 2-10: From left to right a virgin CPGA package, shadow mask for gold coating, gold ground ring evaporated onto CPGA

## Inductively Coupled Plasma

Inductively coupled plasmas (ICP) use an RF inductive element to couple energy from an RF power source to an ionized gas (Figure 2-11). There are several ways to configure the system to generate inductively coupled plasma [23]. A key feature for the work here is that the inductive element can be separated from the gas by a dielectric window or chamber wall. Inductively coupled plasmas are used on a large scale in semiconductor manufacturing where large wafers are processed in the plasma [24].

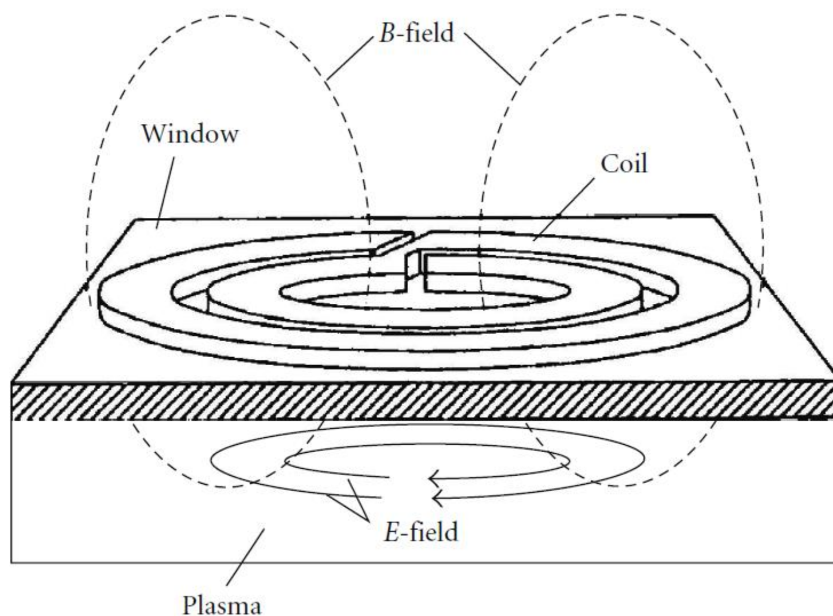


Figure 2-11: Diagram of induced E-field in the plasma [23]

ICP's generate higher density plasmas relative to capacitive discharges at the same RF power. One of the consequences of inductive discharges being high density is a higher ion flux across the sheath. The ion energy and flux in the ICP can be varied independently of each other. The ion flux can be varied by changing the source power

and the ion energy can be varied by changing the substrate electrode voltage. Unlike capacitive discharges, ion energies are only weakly dependent on discharge power and pressure, and are independent of electrode areas [22]. In this case, the electrode of main interest is the ion trap chip. The plasma ions' acceleration energies across the sheath are typically in the 20V to 500V range depending on the electrode bias, and are lower than their capacitively coupled counterparts (Table 2-1).

| | Discharge Type | |
|---|---|---|
| Parameter | Inductive | Capacitive |
| Pressure (mT) | .5-50 | 10-100 |
| Power (W) @ few $cm^2$ | 1.0 - 50 | .5 -20 |
| Frequency (MHz) | 0-1000's | 0.01-10's |
| Density ($cm^{-3}$) | $10^{10}$ - $10^{12}$ | $10^9$ - $10^{11}$ |
| Ion Energies (eV) | 20-500 | 200-1000 |
| Fractional ionization | $10^{-4}$ - $10^{-1}$ | $10^{-6}$ - $10^{-3}$ |

Table 2-1: Inductive plasma parameters vs capacitive, from [22]

The ICP for this work is a small-scale plasma source and, therefore, of a slightly different configuration than those used for large-scale manufacturing ICP sources. It consists of a small stove top shaped inductor used to deliver the RF power to the plasma. To achieve a smaller plasma in the application here, the coil was scaled down [25]. The inductive coil was formed using 10 gauge copper wire that was wound into a two loop spiral with a coil diameter of 27 mm. This diameter was chosen to be just smaller than the diameter of the top of the slot in the shielding plate (Figure 2-12). The ends of the coil are directly connected to the impedance match network. The coil has a copper can covering it

to shield the ambient environment from RF radiation. The shielding plate replaced the metal screen commonly used in surface ion trap experiments. The replacement of the screen with a slotted plate is an advantage in ion trapping experiments as it removes the screen from the line-of-site of the camera that is used to collect photons for ion imaging. This plate can be held at ground potential or (in principal) biased to modulate the ion energies from the plasma to the surface of the trap. For plasma cleaning, in the ion trapping experimental chamber, the photon collection optic (lens) is removed from the re-entrant viewport and the inductor is placed directly above the window in the re-entrant port (Figure 2-13). When the RF power is applied to the coil a magnetic field extends through the window and induces an electric field in the ionized gas to initiate and maintain the plasma (Figure 2-11).

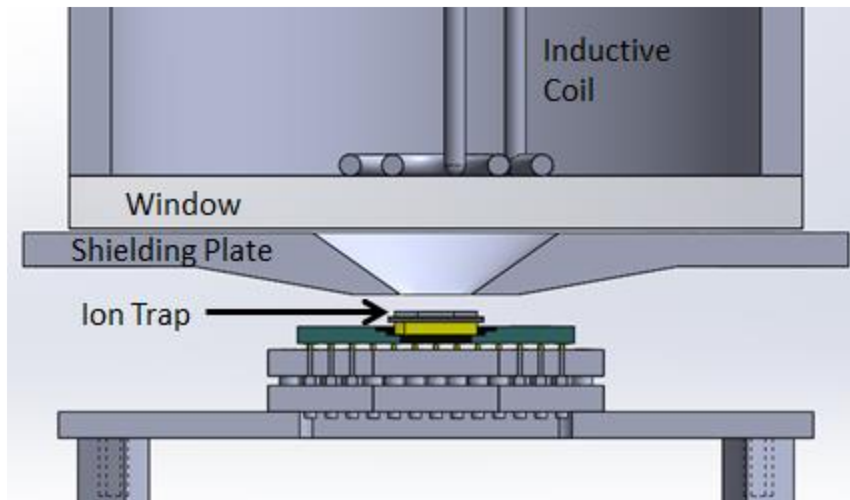


Figure 2-12: Configuration for inductively coupled plasma

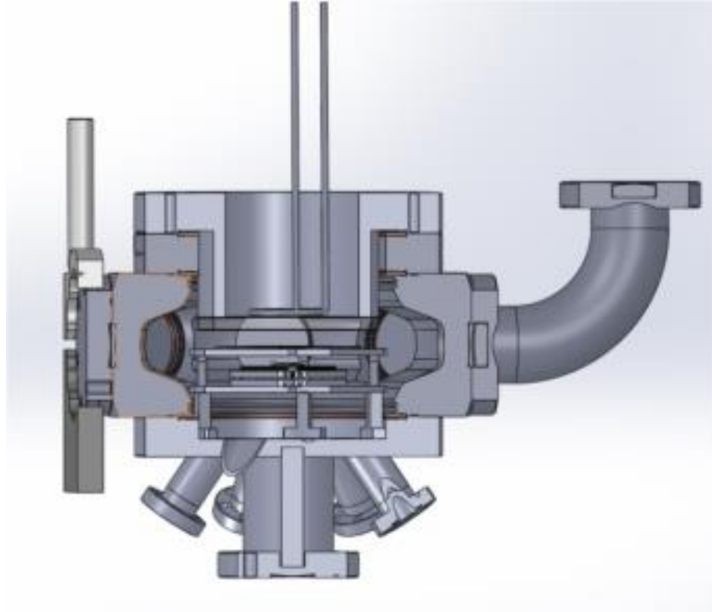

Figure 2-13: Ion trapping chamber shown with RF plasma coil on re-entrant viewport.

## Retarding Field Ion Energy Analysis

The energy of the ions arriving at the surface determines the ability of plasma ions to clean and/or modify the surface. For the objectives of this work, it is critical to know if the surface contaminants are being removed by the treatment process. It is also important to know if the metal is being sputtered by the plasma. There are two concerns with removing the metal. First, the metal could redeposit between the device electrodes causing electrical shorts and rendering the trap useless. Second, if the sputtered metal coated the viewport it would obstruct the light collection from the trapped ion. Furthermore, it could be detrimental to the trapping experiment if the glass viewport is clouded or etched by the plasma ions.

Finished RFA

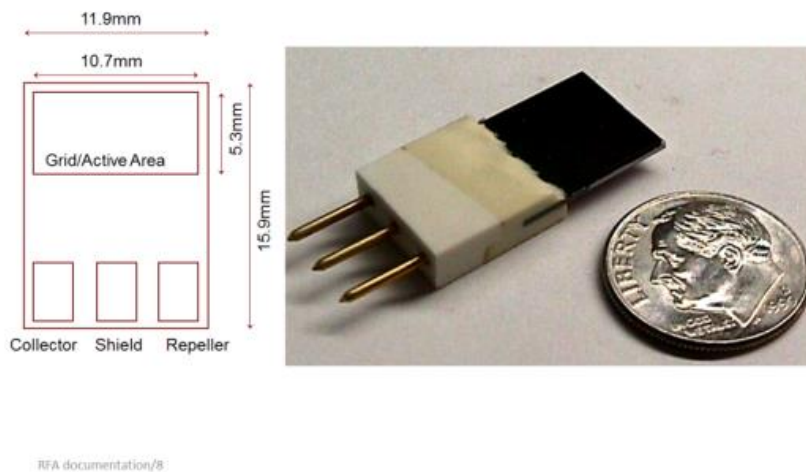


Figure 2-14: Packaged retarding field energy analyzer.

A retarding field energy analyzer (RFA) was used here to determine the ion energies arriving at the surface of the ion trap (Figure 2-14). The RFA was designed and fabricated for characterizing ICP’s in semiconductor plasma processing chambers [26]. The analyzer has three plates as seen in Figure 2-15 and Figure 2-16. There are holes in the top plate that allow plasma ions and electrons to pass through. The top plate acts as a shield to the other two plates by screening the plasma potential from the potentials of the lower two plates. The shield can be grounded or left floating. Since it is the ion energies that are of interest, the middle plate (the repeller), is biased negative to reject all incoming electrons. The third plate is the collector and receives the ions from the plasma. Holes in the shield and repeller are self-aligned to minimize error in the measurement. Furthermore the diameter of the hole is smaller than the sheath distance, so differential pumping is not necessary and the plasma does not enter the analyzer.

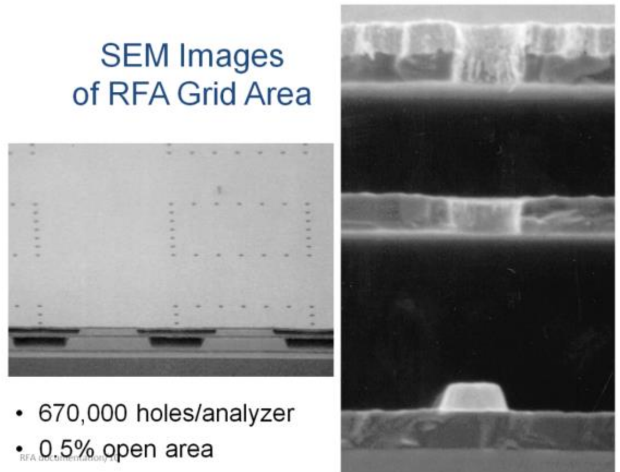


Figure 2-15: Cross-sectional images of retarding field energy analyzer.

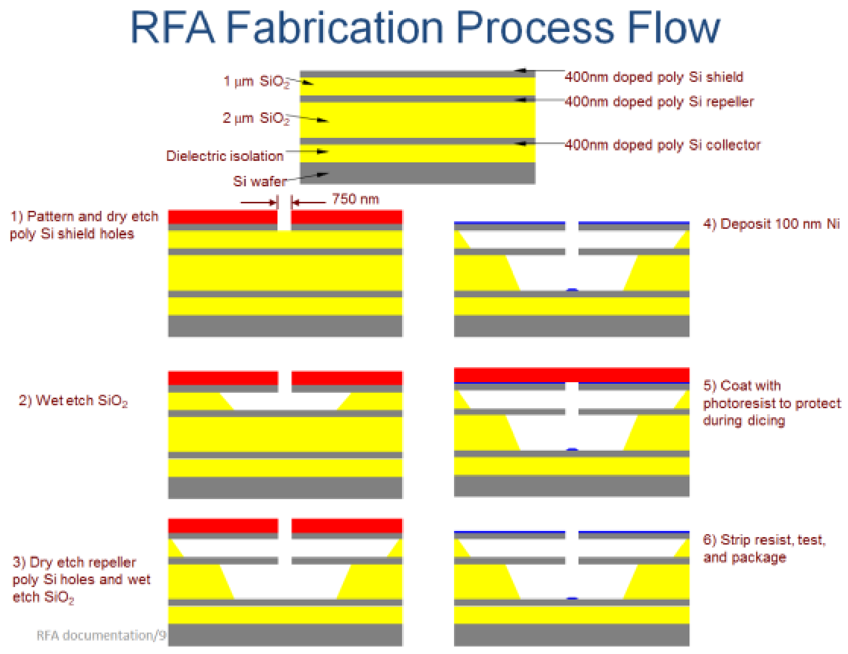


Figure 2-16: Process flow for retarding field energy analyzer.

To determine the appropriate bias voltages of the analyzer and extract the ion energy distribution, a range of voltages first is swept across the repeller and the collector in the presence of a plasma in order to determine the potential to be fixed at the repeller.

First, the collector is held at zero volts and the current is measured using a Keithley 6487 picoammeter voltage source as the repeller voltage is swept starting from zero volts going negative until the current measured on the collector saturates (Figure 2-17). The saturation of the current means all plasma electrons are being rejected and only plasma ions are contributing to the current on the collector. After the repeller voltage is set, the voltage on the collector is scanned in the positive direction. As the voltage on the collector becomes higher than the ion energies entering the analyzer, the current on the collector drops to a minimum (Figure 2-18). This current vs voltage curve is then differentiated to give the ion energy distribution (Figure 2-18).

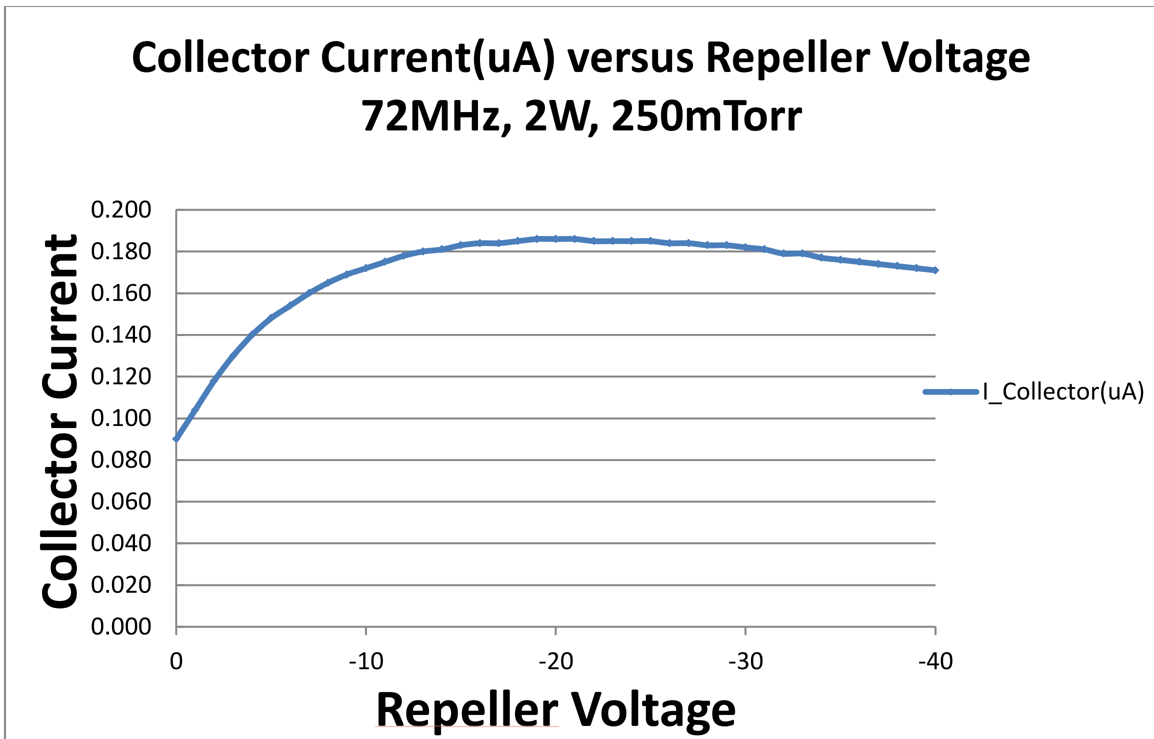


Figure 2-17: Repeller scan.

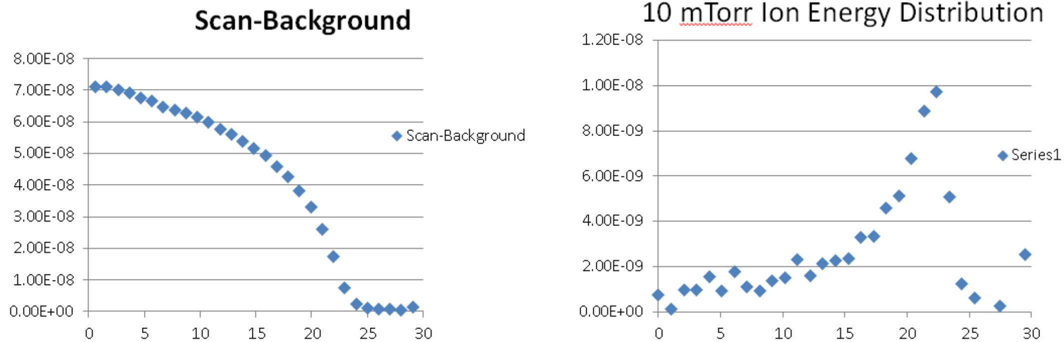


Figure 2-18: Collector scan and ion energy distribution.

In the plasma test chamber, the RFA was inserted in the place of the trap chip. The screen and the shielding plate were removed to allow ample space for the plasma to be generated.

## X-ray Photoelectron Spectroscopy

A critical measure of the efficacy of plasma removal of surface contaminants is their nature and amount. There are many analysis techniques for determining chemical composition on surfaces. A few of these surface analysis techniques are Auger electron spectroscopy (AES), X-ray photoelectron spectroscopy (XPS), and secondary ion mass spectroscopy (SIMS). In AES, electrons are accelerated at the surface of the sample and Auger electrons are detected revealing the chemical composition of the surface. If care is not taken in limiting current density of the electron beam while using AES, it can induce surface modifications through Electron Stimulated Desorption (ESD) [27]. In XPS, an X-ray source is directed at the sample, electrons are collected on a detector and the amount of surface damage is reduced [28]. AES and XPS are both surface analysis techniques

that probe the top few nanometers of a sample. SIMS is a technique that sputters the top 1-2 nm of the surface and analyzes the ejected secondary electrons. SIMS is the most sensitive surface analysis technique with detection limits ranging from parts per million to parts per billion.

In this work, a Kratos Axis Ultra DLD XPS is used to determine the surface composition. A key reason for using XPS in this work is that it has less potential for modifying the surface during the analysis and it gives quantitative results (in atomic %) for surface contaminants. The XPS tool is equipped with a vacuum load lock where samples are introduced into the system. The load lock is isolated from the analysis chamber by a gate valve allowing samples to be inserted without venting the analysis chamber to atmosphere. A transport arm is used to move the sample from the load lock to the analysis chamber. Once the sample is aligned and the area on the device under test is identified, an X-ray source is turned on. The X-rays cause photoemission of electrons which escape from the top 0-10 nm of the surface. An electron energy analyzer separates the electrons by their kinetic energy and they are counted by the detector. Due to photo-electric effect the energy of the electrons emitted from the surface is directly related to the chemical species on the surface of the sample.

The ion trap plasma test chamber was slightly modified to interface to the XPS chamber via the load lock. One of the viewports on the chamber was removed and a magnetic transfer arm was attached in its place allowing a sample to be transferred from the plasma chamber to the load lock of the XPS. The socket that receives the ion trap chip package was also removed and the sample (trap chip) was placed directly on the magnetic transfer arm.

The XPS experiments were conducted as follows. A sample was loaded into the XPS tool and a pre-plasma exposure XPS scan of the sample was saved. The sample was then transported via the transfer arms into the plasma chamber where it was treated with plasma. Without returning to atmosphere the sample was transported back to the XPS chamber and post-plasma XPS measurements were made. The pre- and post-plasma scans were compared to determine the effect of the plasma exposure on the sample surface.

In this chapter, the experimental setup was presented explaining the devices and instruments used to perform the necessary experiments. Different plasma approaches were presented and plasma diagnostic techniques were explained.

# Chapter 3

# Results and Discussion

The first experimental objective in integrating a plasma discharge capability with an ion trapping experimental chamber was to determine if a UHP gas could be introduced into the trapping chamber and then pumped out to achieve UHV. Then, proof of concept experiments were conducted showing that plasma can be generated in the ion trapping chamber. CCP and ICP configurations were explored and results presented. The main goal of this work was to implement an *in situ* surface cleaning solution which did not modify the ion trap electrode surface metal. This goal was achieved. An advantage of the solution presented here is the minimal changes necessary to an ion trapping chamber for implementation on a working ion trap experimental chamber.

## Vacuum Pressure Test

Tests were performed to establish that the chamber could be returned to UHV conditions after introducing UHP gas for plasma cleaning. For an *in-situ* cleaning solution to be a viable option in this application, it is important that a UHV pressure can be recovered post treatment without the need to re-bake the chamber. For ion trapping experiments, pressures in the range of $10^{-10}$ Torr and below are necessary. Furthermore, it is undesirable to fire the titanium sublimation pump, as the pressure rises dramatically during firing, and contaminants burned off the titanium elements could reach the ion trap surface.

A simplified vacuum chamber (Figure 3-1) was constructed using only the necessary components for the test. The leak valve, MKS (vacuum gauge), ion pump, ion gauge, titanium sublimation pump and the bakeable valve were assembled to a 2.75” cross using the same rigor as an actual ion trapping chamber. After cleaning and assembling these components, this test chamber was baked at 200 ºC for five days while pumping with a turbo molecular pump (TMP), after which the bakeable valve was closed. The final base pressure of $1\times10^{-12}$ Torr was achieved using the ion pump and the titanium sublimation pump.

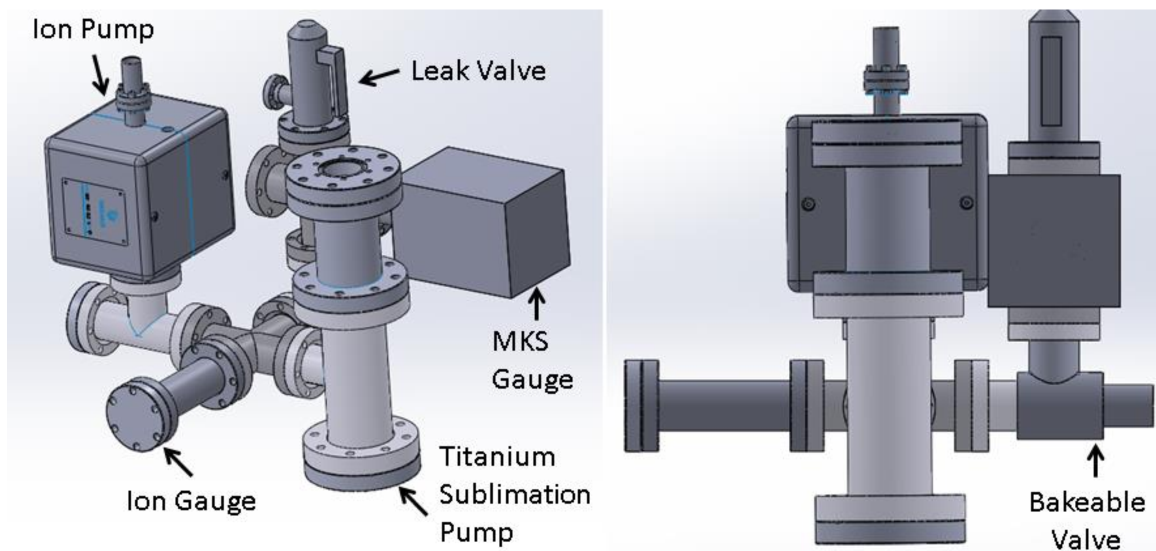


Figure 3-1: Drawing of simplified chamber for UHP gas introduction test

A bottle of UHP gas (10% oxygen semi 4N5 / argon ULSI 6N) was attached to the chamber using a clean manifold. This manifold had also been baked and evacuated using a TMP. The base pressure of the manifold was $1.7\times10^{-8}$ Torr. The bakeable valve on the chamber was opened and the UHP gas was leaked into the chamber to a pressure of 1 Torr, which was estimated to be at the higher end of the pressure range that would be

used for running the plasma discharge in an ion trapping chamber. The gas was then pumped out using the TMP. When the MKS gauge read $9.7\times10^{-9}$ Torr, the bakeable valve was closed and the ion pump was turned on. After 16 hours, the pressure on the ion gauge inside the chamber read $6\times10^{-12}$ Torr, well within the pressure range for trapping ions.

A similar test on an experiment-ready ion trapping chamber using UHP (99.9999%) argon did not yield similar results. The base pressure of the chamber was $5.5\times10^{-11}$ Torr. Argon was introduced up to 250 mTorr and allowed to flow through the chamber for 10 minutes after which the chamber was evacuated. The vacuum pressure after the test was $1\times10^{-10}$ Torr. This higher pressure is attributed to the much larger surface area inside the experiment-ready chamber. Ion heating rate measurements can be performed at this pressure; therefore work to reduce the pressure further was not pursued.

## Capacitively Coupled Plasma

For *in situ* plasma cleaning to have the greatest utility, the implementation must not interfere with other aspects of the ion trapping experiments. CCP was initially investigated to see if plasma localized above the trap surface could be quickly implemented by simply adding a feedthrough for plasma RF and an additional bakeable valve for gas flow.

The proof of concept CCP was implemented by applying RF to the screen in the trapping chamber. Argon gas was introduced into the chamber to reach a pressure of $1.4\times10^{-2}$ Torr and RF power of 5 W at 13.56 MHz was applied. The resulting plasma discharge was diffuse, filling the whole chamber (Figure 3-2) and, therefore, did not meet

the requirement for localized plasma. However, it was established that plasma could be easily implemented in the ion trapping chamber.

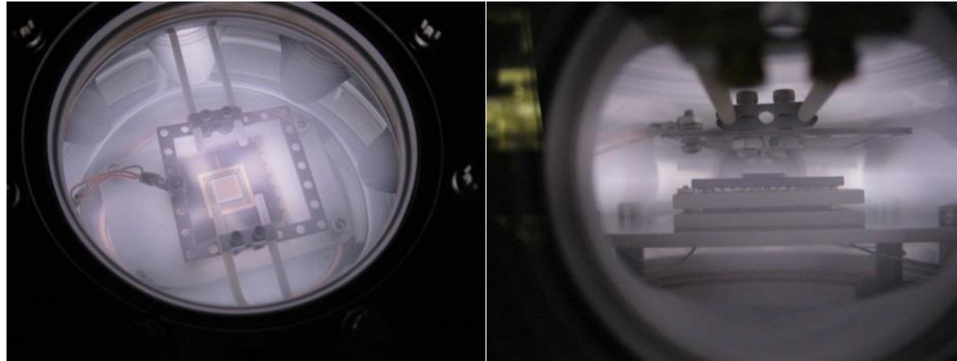

Figure 3-2: Diffuse plasma in test chamber, low millitorr pressure about 20 W

To localize the plasma, the seal ring of the packaged ion trap was used as the RF driven electrode. Ideally, the plasma is to be over the electrode area of the trap chip, and not at the edges of the chip or anywhere else in the chamber. Initially in the plasma test chamber other grounded surfaces near the unshielded RF wire and near the trap were present, allowing stray RF fields and plasma formation in other locations of the chamber. Stray RF fields were mitigated by using a shielded coaxial cable with SMA connectors on both ends helping to localize the plasma around the ion trapping chip as shown in Figure 3-3.

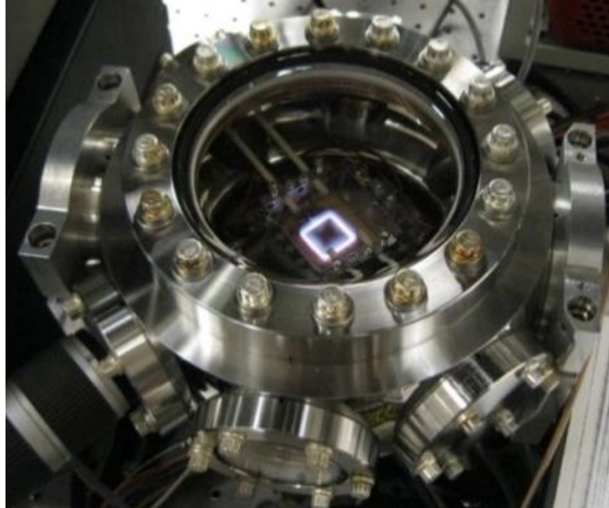

Figure 3-3: Localized capacitive plasma appears to not cover the center of the ion trap.

An ion trap was prepared with an SMA connector, as previously described, and installed in the ion trapping experiment chamber. UHP oxygen-argon gas was introduced into the chamber to a pressure of 1 Torr. RF power of 4 W at 17.9 MHz was applied and plasma was observed in many parts of the chamber suggesting the presence of stray RF fields that were not observed in the test chamber. The post-plasma pressure was $1.7\times10^{-10}$ Torr, high but acceptable for ion trapping experiments.

CCP exhibited some undesirable characteristics, principal among them being that the plasma was not confined in the ion trapping chamber as it was in the test chamber. Additionally, in the test chamber after many multiple plasma treatments, a 1 kΩ short developed between the plasma RF and the ground electrode due to sputtered gold (Figure 3-4). This was visually confirmed by observation of re-deposited gold on the ceramic chip carrier. This shows that the ion energies were high enough to sputter the trap surface which is consistent with CCP theory, in that ion energies are dependent upon plasma

power, pressure, and area ratio of electrodes and can be in excess of 1 keV. These phenomena are not acceptable for the subsequent trapping experiments.

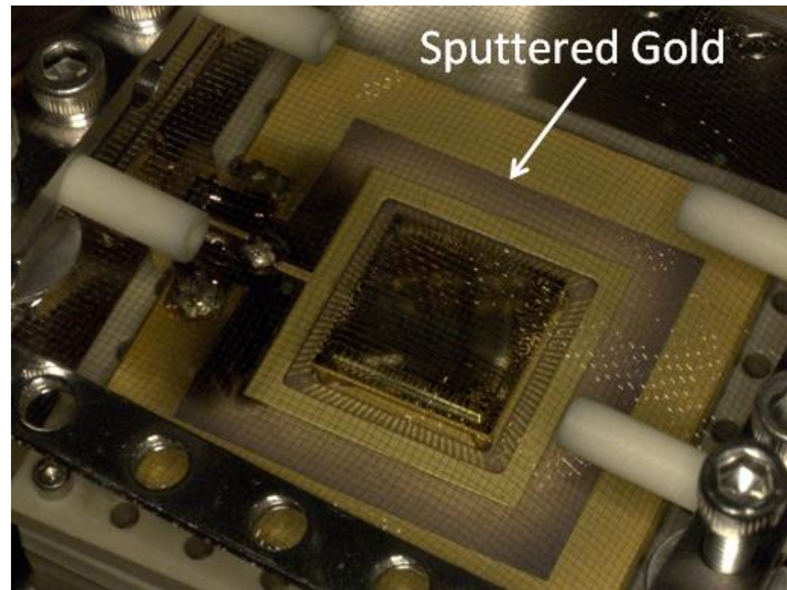


Figure 3-4: Sputtered gold from high ion energies

Other CCP configurations were discussed for successfully confining the plasma and controlling the ion energies at the device surface (Figure 3-5). One such configuration would be to confine the plasma between two screens and bias the device surface to control ion energies.

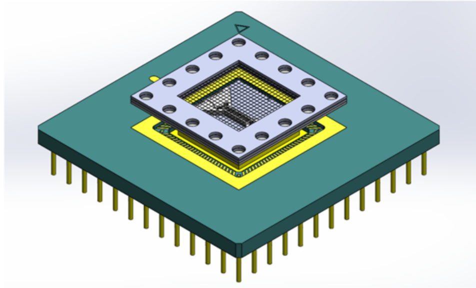

**For capacitive discharges:**

**Area ratios matter**

**Asymmetric capacitive discharges lead to voltage imbalances due to differences in electrode areas**

**For a collisional sheath (higher pressures)**

$$V_a/V_b = (A_b/A_a)^{5/2}$$

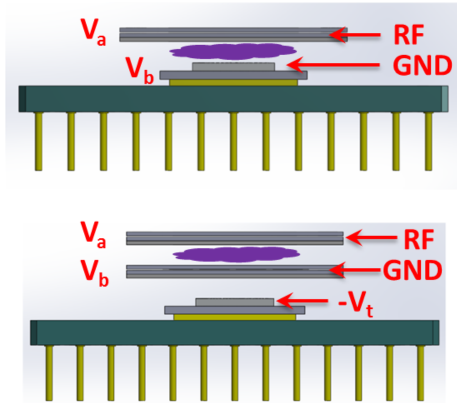


**Case 1**

$$\frac{V_a}{V_b} < 1$$

**Case 1: Ion energies arriving at trap rely on plasma conditions only**

**Case 2**

$$\frac{V_a}{V_b} = 1$$

**Case 2: Ion energies arriving at trap rely on bias voltage $V_t$ on trap**

Figure 3-5: Capacitively coupled plasma discharge configurations.

While the capacitive discharge proved the concept of generating plasma in an ion trapping chamber, it proved challenging to localize. Therefore, inductive plasma generation was investigated.

## Inductively Coupled Plasma

ICPs are driven by the induced electric field from the resonator. The size, location and applied power of the resonator greatly affect the plasma volume, so tuning these parameters can lead to a localized plasma. Additionally, ion energies are generally much less than 100eV and are decoupled from the plasma power, pressure, and area ratio of electrodes. As mentioned previously, inductive plasmas are used in CMOS processing and larger ion energies are achieved and controlled by (RF) biasing the sample substrate.

For this work, another attractive attribute of ICP is that the RF power can be delivered external to the chamber, thereby minimizing internal chamber modifications.

The industry standard for exciting RF plasma is 13.56 MHz and these systems generally operate at hundreds to thousands of watts for establishing plasmas in relatively large process chambers. For this application, it was necessary to generate a localized small-volume plasma and it was found that the frequency needed to be increased and the power decreased. Work done by Yin *et al.* [25] on miniature ICP sources gave great insight into this process. The plasma density and volume are related to the power applied. The induction electric field decays exponentially within the plasma[29]; with a low enough field the plasma is localized. For the work here, it was found that 72 MHz is the (nominal) frequency at which the best impedance match was achieved with the lowest initiation power. The configuration shown in Figure 3-6 achieves the desired result of localized plasma (Figure 3-7).

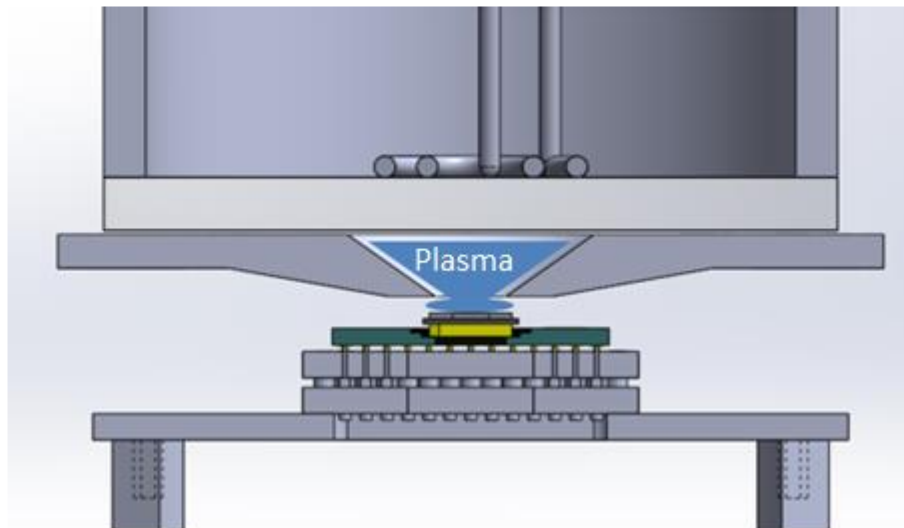


Figure 3-6: Inductively coupled plasma setup.

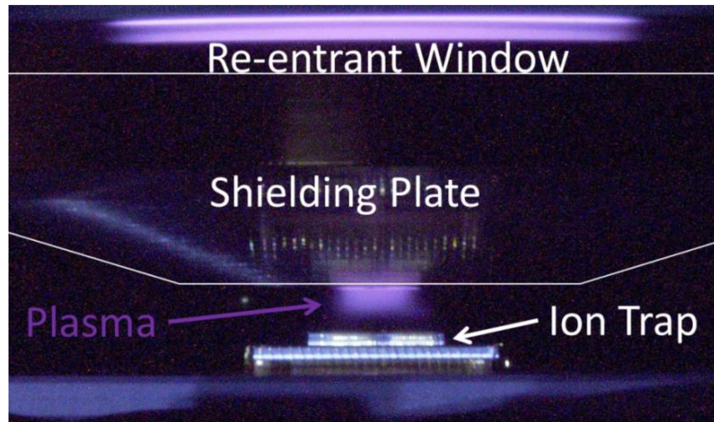


Figure 3-7: Image of localized plasma directly above the ion trap surface in the ion trapping experimental chamber.

The initiation power vs pressure curve (Figure 3-8) was used to find the optimal operating conditions for plasma treatment in the ion trapping experimental chamber.

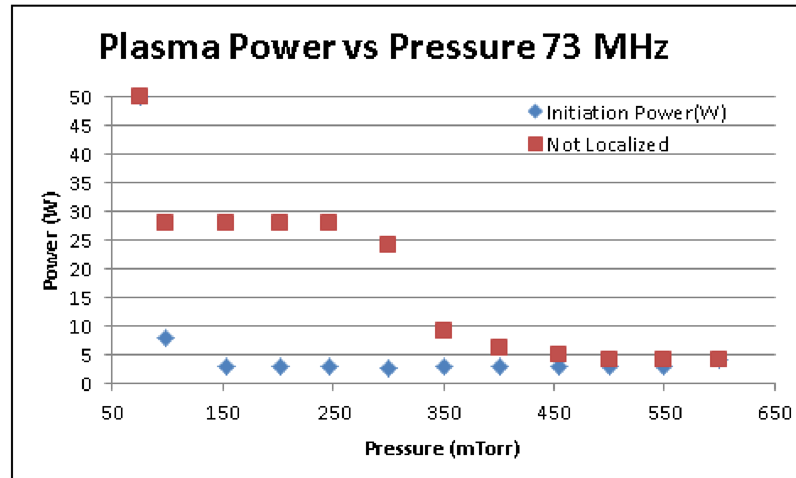


Figure 3-8: Initiation power vs. pressure curve.

## Ion Energy Measurements

There are many methods to characterize plasma conditions including UV-visible spectroscopy, electric (Langmuir) probes, and retarding field energy analyzers (RFAs).

Since the ion energy is the primary parameter of interest in this work, an RFA as described in [26] was used to characterize the plasma.

Plasma was initiated at 72 MHz with a forward power of 1 Watt. The ion energy distribution was obtained by applying -30 volts to the repeller, sweeping the collector voltage positive, and then taking the derivative of the current vs voltage measured from the collector (Figure 3-9). The maximum measured ion energies were around 20eV at pressures from 10 to 50 mTorr, which is consistent with literature (Figure 3-10) [26]. The slight shift of the peak distribution to lower energies as the pressure is increased is attributed to the sheath becoming more collisional at higher pressures. The broadening of the ion energy peak at 40 and 50 mTorr is also attributed to a more collisional sheath.

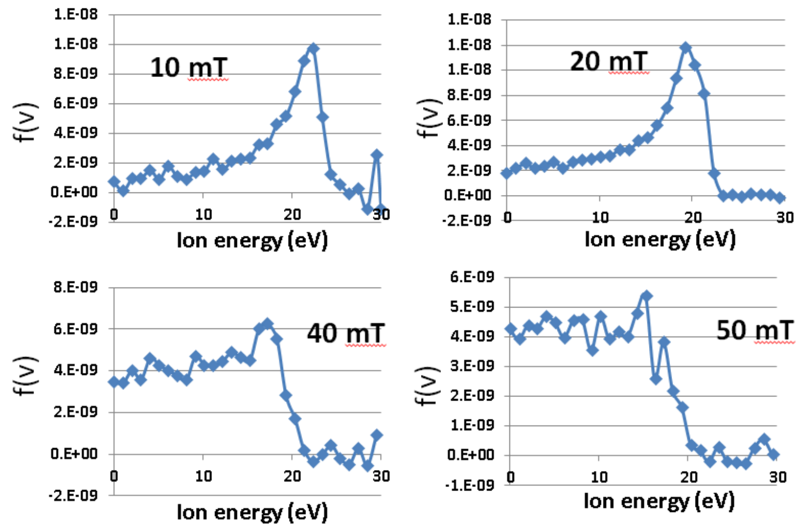


Figure 3-9: Ion energy distribution, $P_{rf}$ = 1W, $\Omega_{rf}$ = 72 MHz, Retarding Field Analyzer Repeller = -30V

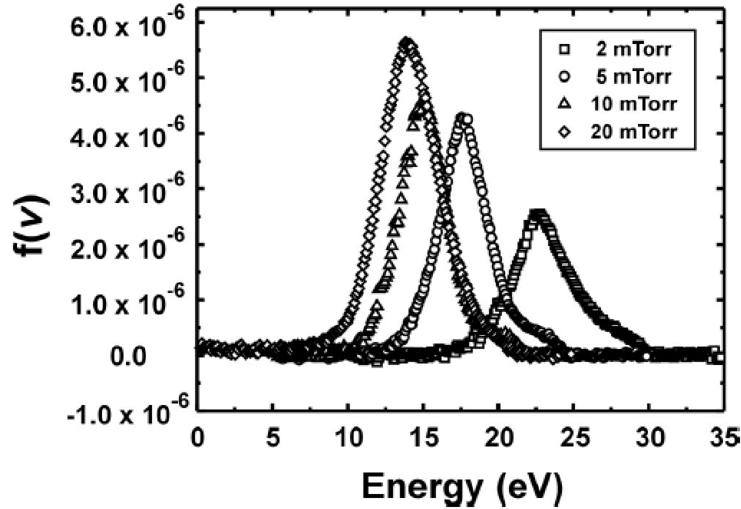


Figure 3-10: Ion energies for various pressures [26].

From the literature, it is found that surface adsorbate bond energies are less than a few electronvolts and, therefore, low energy ion bombardment should, in principle, remove these contaminants without appreciably modifying the underlying surface [30]. The surface contaminants are primarily adventitious carbonaceous species [11] from exposure to atmosphere. It was found in [31] that the desorption energy of CO on gold ranges from about 0.2 eV to 0.57 eV as the surface coverage gets thinner, because the surface potential goes up as more carbon is liberated from the surface.

Whenever energetic particles impinge on a surface with a high enough energy there is erosion of the surface; this process is called sputtering. Sputtering of materials is widely used in semiconductor manufacturing. One such sputtering method is plasma processing described in [32]. Sputter yields by noble gas ions have been extensively investigated. The sputter yields of gold by low-energy argon ions can be seen in Figure 3-11. From [16], an empirically derived sputter yield function is given by

$$Y = a(1 - \sqrt{E_0/E})^{\frac{5}{2}}[1 + b(\sqrt{E/E_0} - 1)] \qquad (1)$$

where Y is the sputter yield, E is the energy of the ion and a, b and $E_0$ are constants. It can be seen in Figure 3-11 that the sputter yield is much less than 0.1 for the ion energies in the plasma generated for this work.

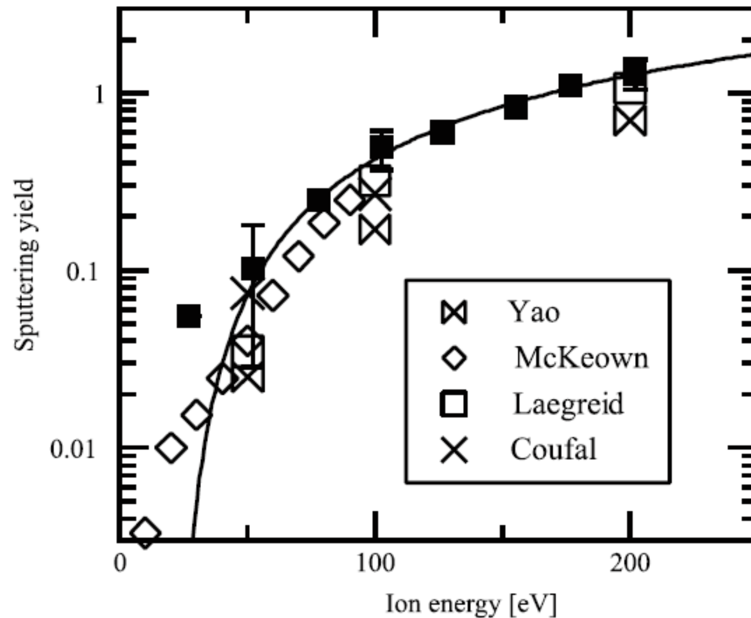


Figure 3-11: Sputter yields for low energy argon ions [16]

The ion energies measured here along with the results from the literature indicate that it should be possible to establish an ICP that has ion energies that are high enough to remove surface adsorbates yet below the sputter threshold of the surface material.

To prove this hypothesis, the surfaces of prepared samples were characterized using XPS before and after exposure to plasma treatment. The samples were surface electrode ring trap chips [18] with half the surface gold coated (Figure 3-12), and the other half aluminum coated. Pre-plasma XPS data measurement on the gold side of the trap chip showed XPS peaks of gold, carbon and oxygen. The pre-plasma XPS scans can be seen in Figure 3-13 and Figure 3-14. The results show the atomic concentration of

carbon on the gold side of the sample to be around 30 % for all samples (Table 3-1). The outliers are samples #2 and #3. Sample #2 came from a different wafer and it was stored in a different waffle pack from the rest. Sample #3 had been exposed to a capacitively coupled argon discharge routinely used for sample preparation prior to wire bonding (the other samples were not). The ion energies in this (packaging related) capacitive discharge are high enough to sputter the surface metals which can re-deposit across the trap. Although gold does not form a native oxide, the presence of oxygen on the samples is not un-expected since some of the carbon contamination from the atmosphere is in the form of $CO_2$ [31].

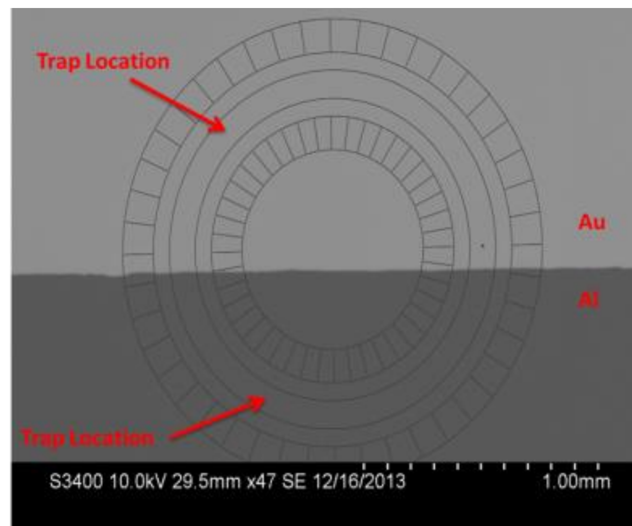


Figure 3-12: SEM image of ring-shaped ion trap with gold on half of the trap surface and aluminum on the other half.

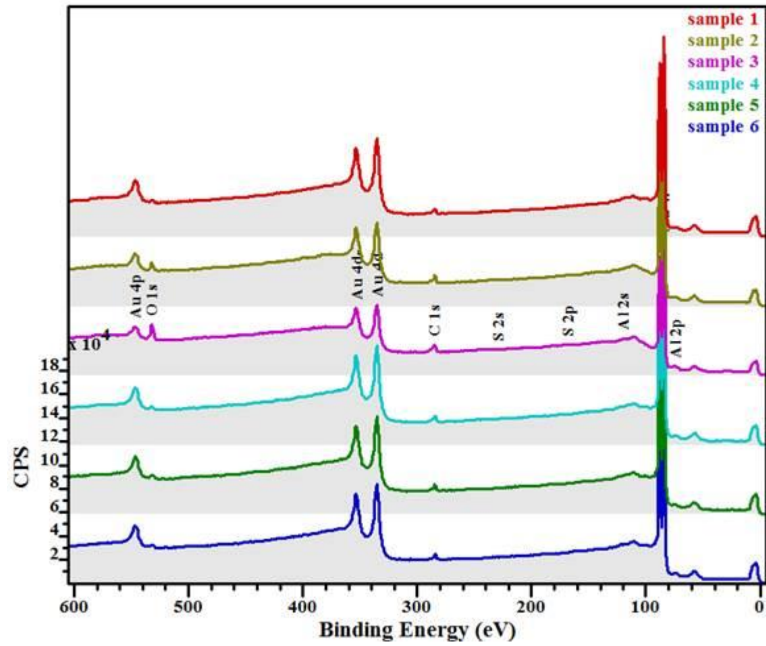


Figure 3-13: Pre-plasma XPS scan on the gold side of samples 1 through 6

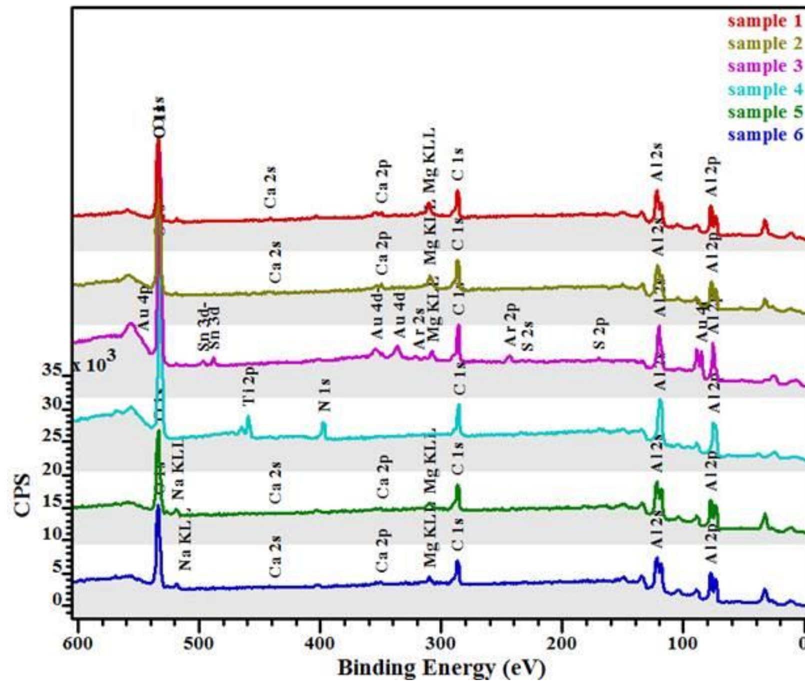


Figure 3-14: Pre-plasma XPS scans on the aluminum side of sampes 1 through 6

| Pre-plasma treatment Gold Side Atomic Concentration (%) | | | | | |
|---|---|---|---|---|---|
| Sample# | Al | Au | C | O | other |
| 1 | 0 | 62 | 33 | 5 | 0 |
| 2 | 0 | 55 | 32 | 13 | 0 |
| 3 | 4 | 32 | 37 | 26 | 0 |
| 4 | 0 | 69 | 26 | 5 | 0 |
| 5 | 0 | 66 | 28 | 6 | 0 |
| 6 | 0 | 63 | 31 | 6 | 0 |

Table 3-1: Pre-plasma treatment concentrations by atomic percent taken from XPS scans on the Gold side of each sample.

The first set of samples, #1, #3, #4, and #6, were exposed to various plasma conditions and then returned to a waffle pack for (atmospheric) storage as seen in Table 3-2. Post-plasma XPS scans of these samples showed a reduction in carbon from 26 to 37% pre-plasma (Table 3-1) to 15 to 23% post-plasma see Table 3-3. The data suggests that the plasma removes some, if not all, of the carbon from the surface, with new carbon possibly re-adsorbing during the long exposure to atmosphere prior to XPS analysis. The effect of different plasma parameters was inconclusive.

| Plasma Treatment Conditions | | | | |
|---|---|---|---|---|
| Vplate | Vchip | 30 sec | 300 sec | 1000 sec |
| 0 | 0 | #6 | #3 | - |
| 40 | -40 | #1 | #4 | - |
| floating | floating | - | - | #5 |
| floating | ground | - | - | #2 |

Table 3-2: Plasma treatment conditions, for all conditions the frequency was 72MHz the forward power was 4 W and the pressure was 250 mTorr

| Post-plasma treatment Gold Side Atomic Concentration (%) | | | | | |
|---|---|---|---|---|---|
| Sample# | Al | Au | C | O | other |
| 1 | 0 | 75 | 23 | 2 | 0 |
| 2 | 0 | 79 | 16 | 5 | 0 |
| 3 | 6 | 43 | 17 | 27 | 7 |
| 4 | 0 | 73 | 21 | 6 | 0 |
| 5 | 0 | 82 | 16 | 1 | 0 |
| 6 | 0 | 75 | 22 | 3 | 0 |

Table 3-3: Post-plasma treatment concentrations by atomic percent taken from XPS scans on the Gold side of each sample.

For the next plasma treatment trial, it was attempted to minimize the time after plasma treatment that the sample was exposed to the atmosphere. Samples #2 and #5 were plasma treated and analyzed in the XPS chamber within 30 minutes. The percent carbon on each of these two sample surfaces pre-plasma was 32% and 28% respectively (Table 3-1) and 16% for both samples post-plasma see Table 3-3. While this result does not confirm that carbon was completely removed during the plasma treatment, it strongly suggests that duration of atmospheric exposure of treated samples is a major factor in the atomic concentration of carbon and oxygen post-plasma.

Since adventitious carbon accumulates rapidly at atmosphere during the transfer from the plasma test chamber to the XPS tool, a method eliminating exposure of the sample to the atmosphere was needed for evaluating the effectiveness of the plasma in removing carbon. The time between plasma treatment and XPS analysis also needed to be minimized. Although the XPS tool is in a different lab than the ion trapping chamber, it was possible to move the plasma test chamber to the XPS lab. The XPS system has an extra transfer station just after the load lock and therefore the plasma test chamber, could be attached directly to the transfer station to facilitate in vacuum transfer of samples

using a magnetic transporter (Figure 3-15). This allowed samples to be plasma treated and then transferred to the XPS chamber without being exposed to air.

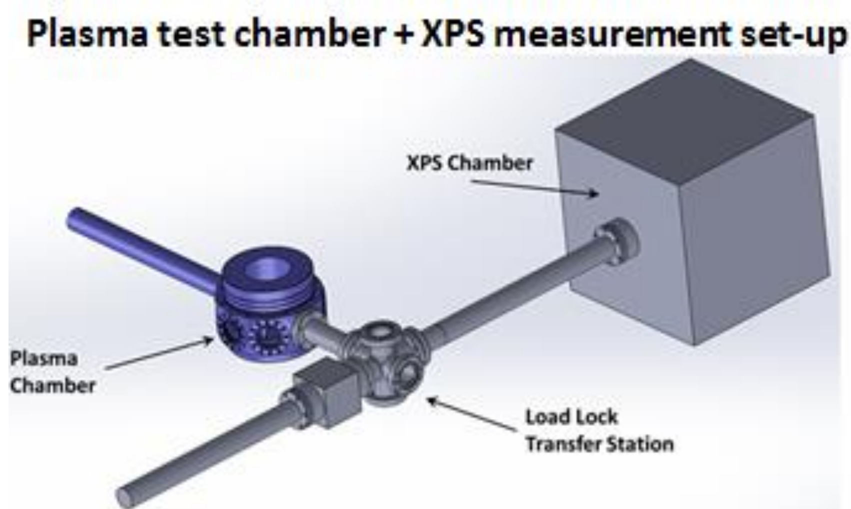


Figure 3-15: Representation of plasma test chamber attached to XPS analysis system.

New trap chip samples were prepared with half the surface electrode ring trap coated with gold (Figure 3-16). For the initial attempts at vacuum transfer of plasma treated samples to the XPS chamber, a sample was attached onto a holder with a small amount of carbon tape which was completely covered by the chip. XPS measurements of sample surface contaminants were taken pre- and post-plasma treatment. Plasma treatment was performed at 72MHz, 4 W power for 5 minutes. Results for these trials showed carbon concentration to be reduced to 9% but not completely removed (Figure 3-17). Although the tape was completely hidden from plasma exposure by the sample, it was speculated to still contribute to the carbon peak post-plasma, as was demonstrated by the subsequent test.

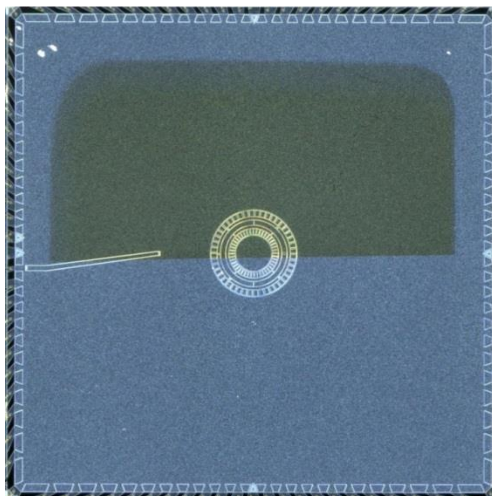

Figure 3-16: Half of the surface electrode ring trap coated with gold.

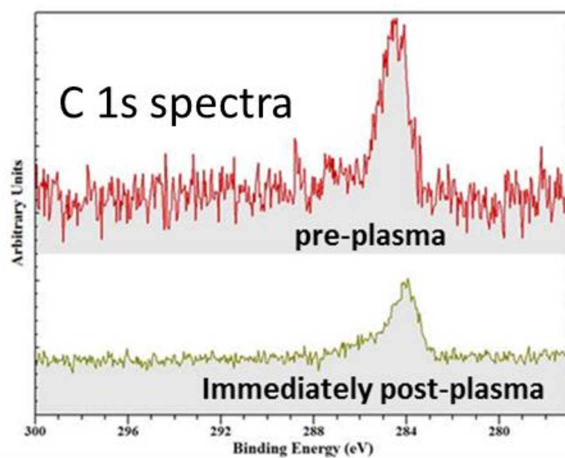


Figure 3-17: XPS results in test chamber, trap chip attached with carbon tape, 5 minutes argon plasma exposure, 4 W, 72 MHz, 250 mTorr.

To completely remove carbon tape, a mechanical sample holder was designed and built to hold the sample. Plasma treatment was performed on a new sample, and the XPS scans pre- and post-plasma were recorded (Figure 3-18). After the plasma exposure, no carbon or oxygen peaks on the gold side of the sample were present. On the aluminum

the carbon percentage was reduced, however, the percent oxygen increased. The increase in oxygen is due to the cleaner $Al_2 0_3$ surface.

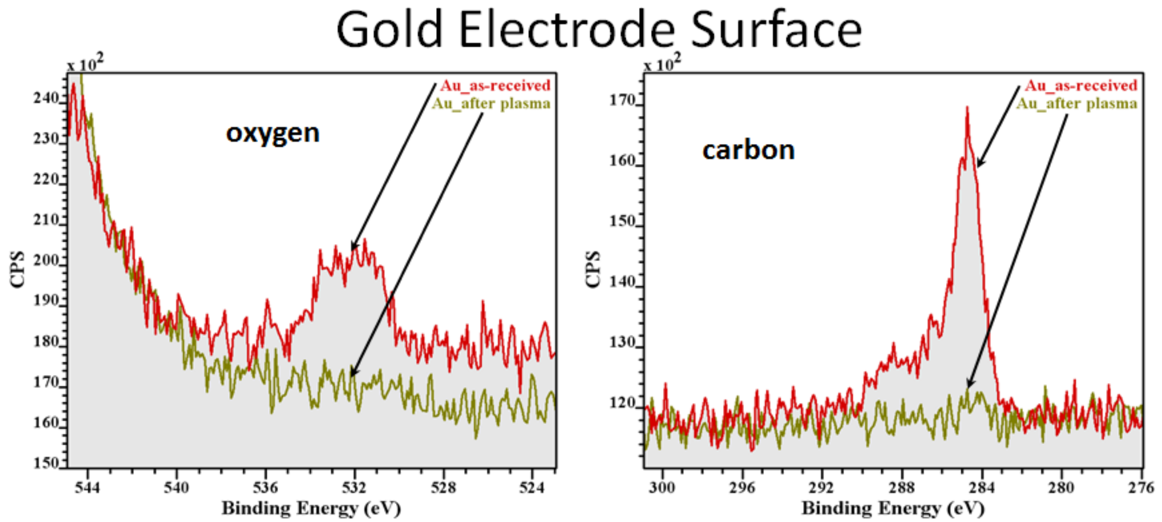


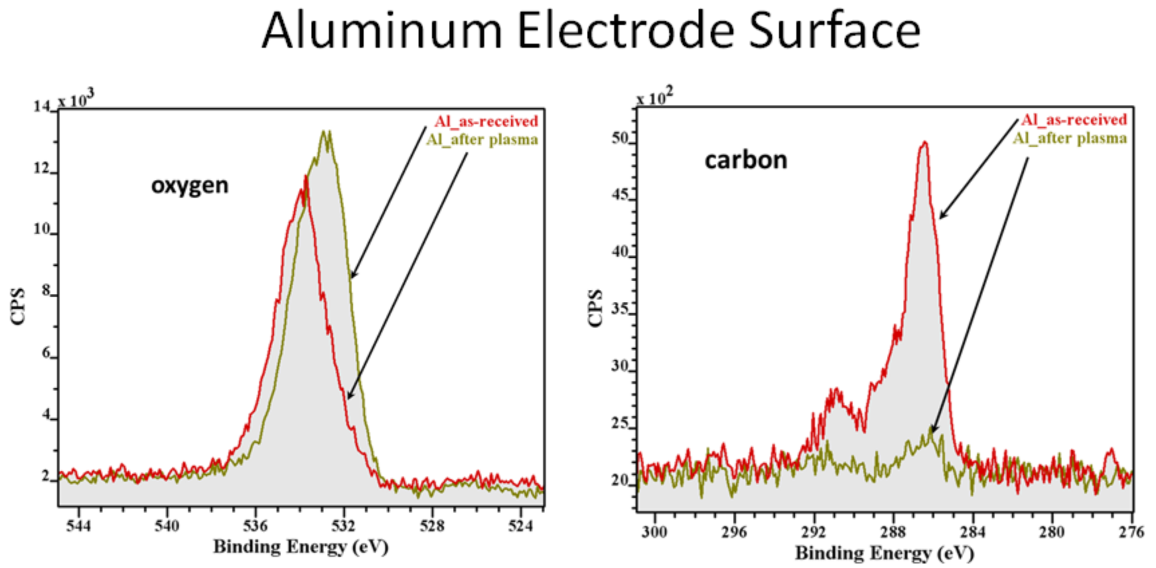


Figure 3-18: XPS spectrum of carbon and oxygen peaks on gold and aluminum surfaces pre- and post-plasma exposure, 72 MHz, 4 W, 300 s.

These data prove the first half of the hypothesis, that the ion energies from the ICP are high enough to remove the carbonaceous species adsorbed on the surface. The second part of the hypothesis is that the plasma ion energies used here are below the appreciable sputter yields of gold by low-energy argon ions. In the XPS scans no gold was observed on the aluminum side and no aluminum observed on the gold side. This validates the hypothesis that the ion energies are below the sputter threshold of the metal on the surface. If a detectable amount of surface metal was sputtered, some re-deposition of the sputtered metal would be expected due to collisions of the metal atoms with incoming argon ions.

It has been shown that localized inductive plasma can effectively remove carbon contamination without sputtering the trap electrodes. The results are summarized in Table 3-4.

| Trials by lab | %Carbon Au side pre-plasma | %Carbon Au side Post-plasma | Notes |
|---|---|---|---|
| Plasma Ion Trap Lab | 31 | 21 | Many Days before XPS analysis |
| Plasma Ion Trap Lab | 31 | 16 | 30min Before XPS analysis |
| Plasma XPS Lab | 36 | 9 | Carbon tape Sample holder |
| Plasma XPS Lab | 35 | 0 | Mechanical sample holder no carbon tape |

Table 3-4: Summary of plasma results by XPS atomic percent carbon.

The next experiment shows that carbon adsorbs on the metal surfaces even at UHV pressures. After plasma exposure of 120 seconds at 250 mTorr, the sample was left in the XPS chamber at a base pressure of $7\times10^{-9}$ Torr overnight with periodic scans. It can be seen in Figure 3-19 that the carbon peak grows over time. These data suggest that the plasma was in fact removing all of the carbon and any small carbon peak observed was adsorbed on the surface during the transfer of the sample back to the XPS chamber, which takes times approaching 5 minutes in duration. During the transfer from the plasma chamber to the XPS chamber the sample was not exposed to atmosphere, but there was some residual carbon in each of the chamber components. These results are also consistent with the post argon ion beam treatment results from the Berkeley experiment [33], where it was shown that over time the carbon peak returns even at UHV pressures.

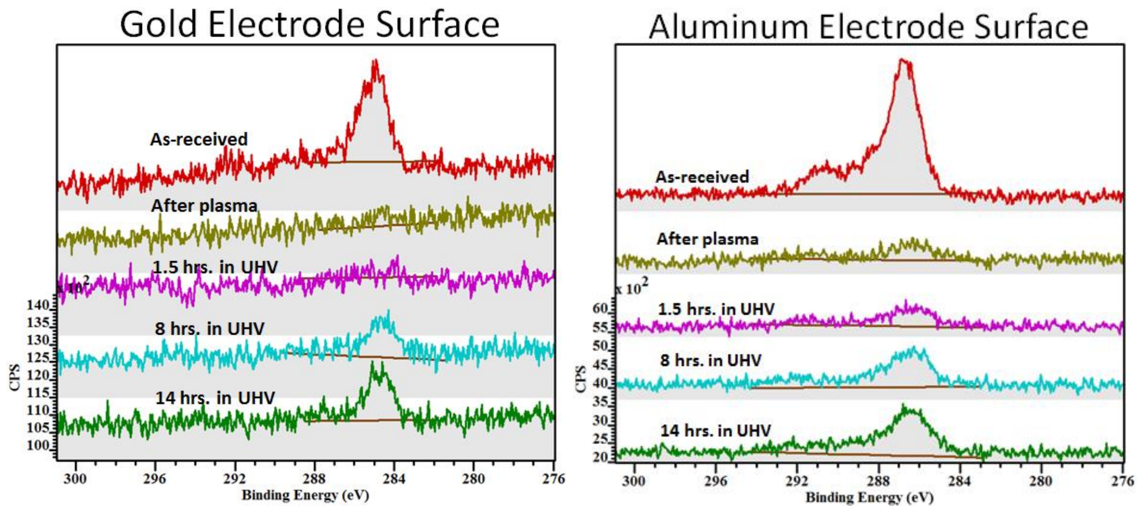


Figure 3-19: XPS spectrum on gold and aluminum pre-plasma and post-plasma showing an increasing carbon peak even while in XPS vacuum chamber including +1.5hrs, +8hrs, +14hrs.

Testing the plasma discharge parameter space revealed that removal of carbon from the surface occurs over a large range of plasma conditions. In these plasma treatment trials three pressures were tried with various times.

Sample exposure to plasma at 250 mTorr was tried for 120 seconds and complete carbon removal was observed. After a 30 second exposure of a new sample, a small carbon peak was still observed, so the same sample was treated for an additional 30 seconds which further reduced the amount of carbon contamination. The resulting XPS scans are presented in Figure 3-20. Analysis at 500 mTorr and 75 mTorr yielded similar results as seen in Figure 3-21 and Figure 3-22.

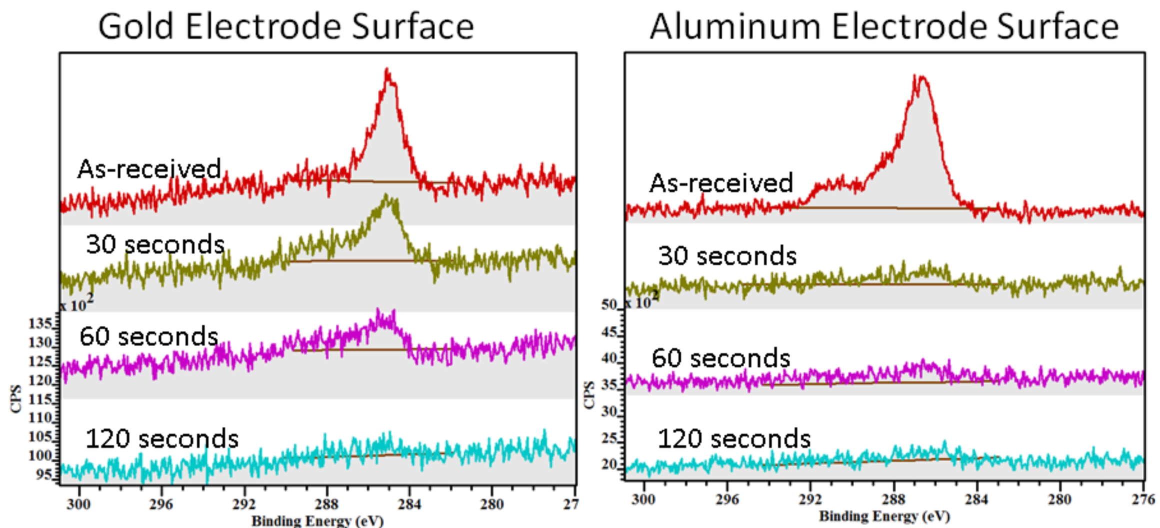


Figure 3-20: Timed plamsa exposure at 250 mTorr, 72 MHz, 4 W

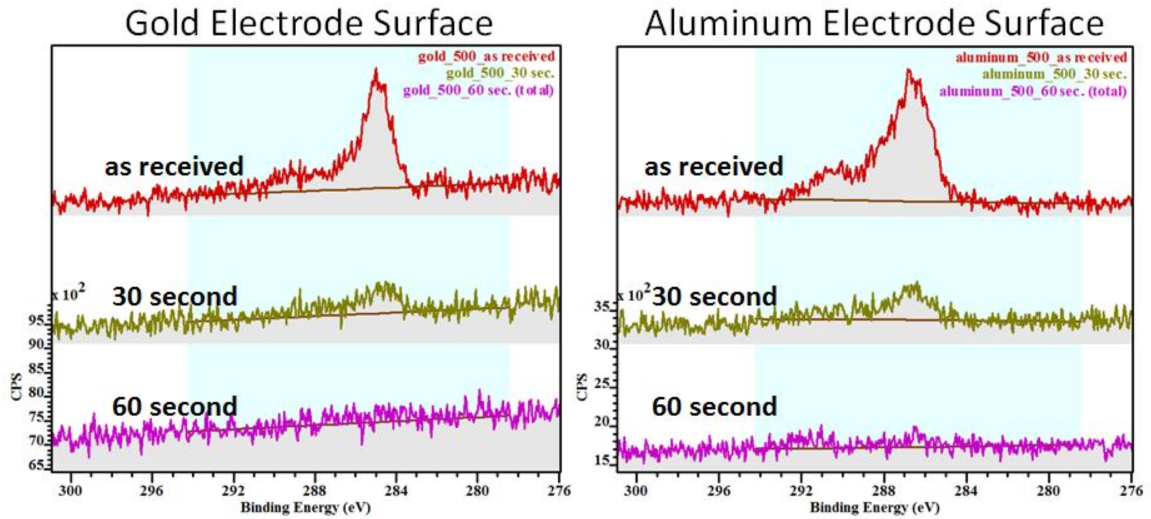

Figure 3-21: Timed plamsa exposure at 500 mTorr, 72 MHz, 4 W

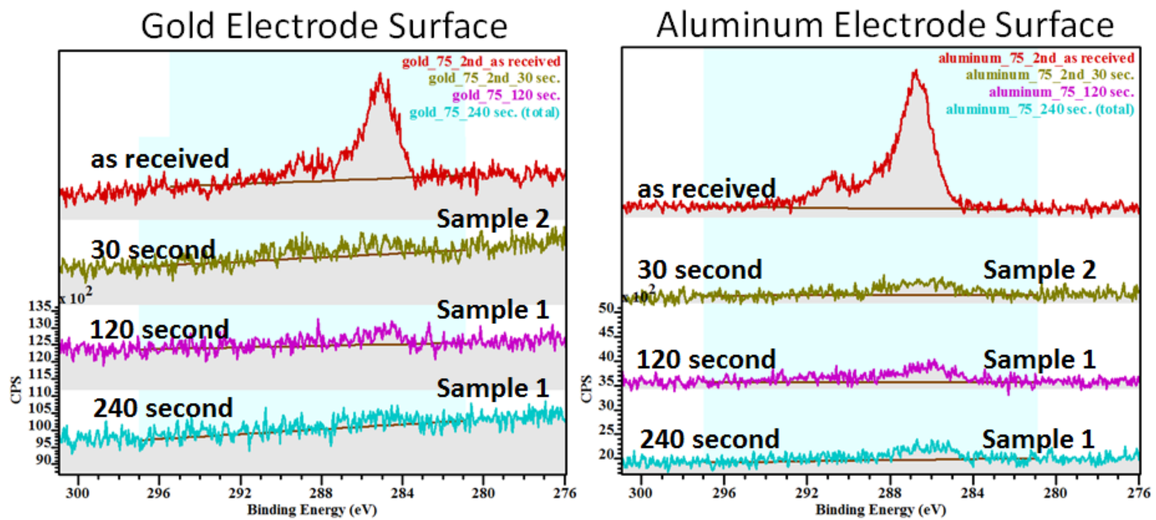

Figure 3-22: Timed plamsa exposure at 75 mTorr, 72 MHz, 4 W

## Heating Rate Measurements

The end goal for an ion trapping experiment is to achieve a low enough ion heating rate that coherent quantum operations can be performed. *In situ* plasma cleaning was performed on a surface ion trap in an ion trapping experimental chamber in order to

determine whether removal of surface contaminants on trap electrodes without modification of the electrode metal via sputter would affect the heating rate.

The ion trap used was a second generation high optical access trap (HOA) designed and fabricated at SNL. It has a narrow isthmus in the center that minimizes laser clipping at the edges of the device (Figure 3-23). The through-chip slot along the center of the device allows for optical access through the chip. An ion can be loaded in this trap either in the center or at one of the four loading hole regions. The loading hole regions are located on each of the arms after the junction region at either end of the slot region.

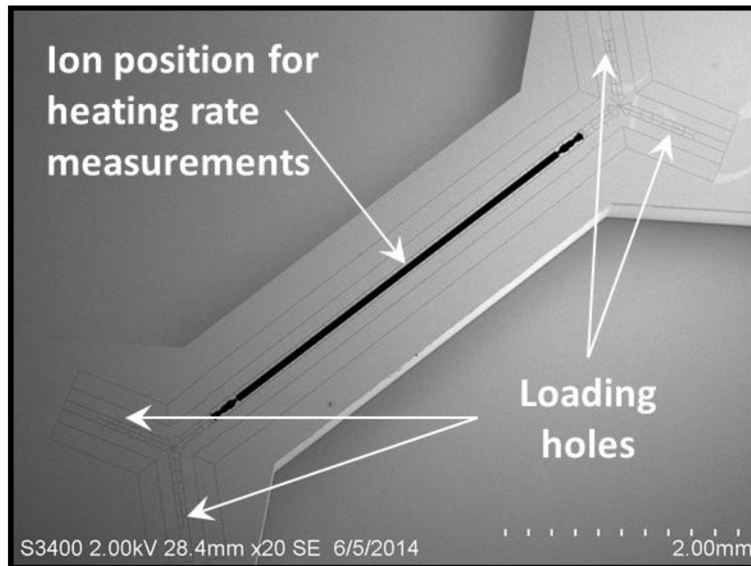

Figure 3-23: HOA2 ion trap chip

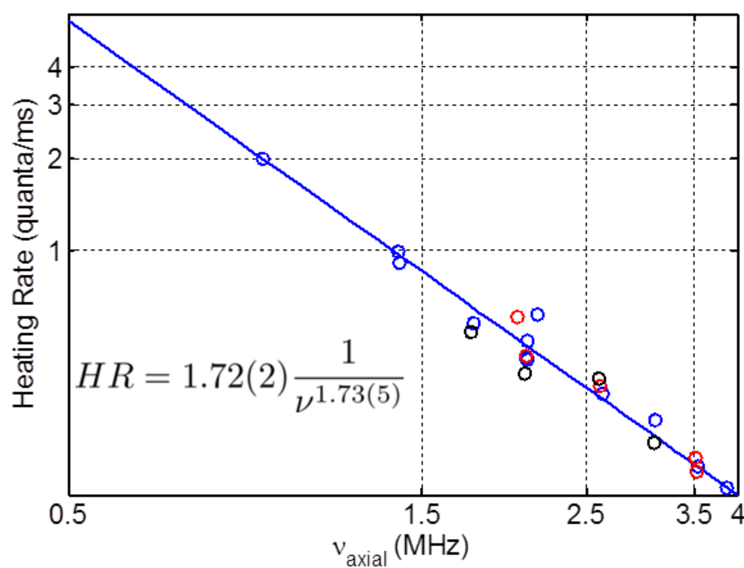


Figure 3-24: Ion heating rate measurements pre- and post-plasma (showing no measureable change). Blue are pre-plasma. Red are post-plasma cleaning trial #2. Black are post-plasma cleaning trial #2.

Heating Rate measurements on the HOA2 device are presented in Figure 3-24. There is a *1/f* dependence that is consistent with other traps where f is the ion axial secular frequency [7]. For an in-depth discussion of ion heating, see the recent comprehensive review by Brownnutt, *et al.* [7]. The first test in implementing plasma cleaning of this trap was to verify that pre-plasma UHV pressures could again be reached after introduction of argon. The argon gas was introduced into the chamber and allowed to flow through the chamber at a pressure of 500 mTorr for 10 minutes. The chamber returned down to $1\times10^{-10}$ Torr in less than 24 hrs, not reaching the starting base pressure of $5.5\times10^{-11}$ Torr, this pressure is acceptable for trapping experimental work.

A first plasma exposure of the trap was performed at a pressure of 250 mTorr with a plasma RF frequency of 72 MHz and a power of 4 W for 5 minutes, after which the base pressure was $3.8\times10^{-10}$ Torr. Measurements of ion heating rates after this plasma

treatment showed no measurable change in the ion heating rate (see the red symbols in Figure 3-24). A second plasma exposure of the sample was performed at 500 mTorr for 60 seconds. After this plasma exposure, argon was flowed through the chamber for 10 minutes in an attempt to more quickly and comprehensively approach the pre-gas-introduction base pressure in the chamber. This post-plasma argon flow decreased the pump down time and the resulting base pressure after the second plasma treatment was $2.5\times10^{-10}$ Torr. Heating rate measurements taken after this second plasma exposure were again found to be within the error bars of the pre-plasma cleaning (see the black symbols in Figure 3-24) showing no measurable change in the ion heating rate.

After the plasma cleaning and heating rate measurements described above, it was noted that the trap chip employed for these tests used epoxy in assembly of the trap chip, interposer chip (which houses RF shunt capacitors and provides redistribution of control line voltages), and the ceramic package. While the bulk of this epoxy is covered by these parts, some was exposed very near the trapping region and was visible to the plasma. Epoxy die attach is a usual method used for assembly of ion traps and has not been shown to adversely affect the chamber pressure. However, carbon liberated by plasma exposure of the epoxy could be deposited onto the trap surface, resulting in little or no change in the concentration of carbon on the trap surface. This source of carbon (epoxy) may have played a similar role as the carbon tape previously mentioned in the XPS plasma experiments.

Future experiments are planned in which no epoxy is present during plasma cleaning. It is suggested that this experiment is required before any concrete conclusions

can be made about the efficacy of plasma cleaning of surface contaminants for reducing ion heating.

# Chapter 4

## Summary & Conclusions

In this thesis the construction and implementation of an *in situ* plasma discharge to remove surface contaminants from electrodes in an ion trapping experimental system was presented with results. Using X-ray photoelectron spectroscopy (XPS) and *in vacuo* transfer of samples between the plasma discharge test chamber and the XPS chamber, it was shown that carbon and oxygen contaminants on the surface of an ion trap can be removed without sputtering the underlying trap electrode. It was also shown that minimal chamber modifications were necessary making this a tractable method for *in situ* cleaning.

Ion heating rates in and ion trapping experiment were measured before and after plasma treatment of electrode surfaces and the observation of no change in heating rates after plasma exposure is attributed to the simultaneous removal and deposition of carbon contamination arising from the (inadvertent) presence of epoxy near the trap. Nonetheless, it was demonstrated that *in situ* plasma treatment of trap electrodes can efficiently remove electrode surface contamination under the right conditions. The results obtained here show that plasma cleaning is a viable way to remove surface contaminants. While more work needs to be done to show unequivocally that removal of carbon is necessary and/or sufficient for reduced heating rates, the results here serve as a basis for further work to understand the role of surface contamination in anomalous heating. This work suggests a plasma cleaning of trap electrodes with no other sources of carbon present (e.g. from exposed epoxy) may prove that carbon removal is necessary but not

sufficient for significant reductions in heating rates. Carbon sources near the trap need to be eliminated and different surface preparations, such as *ex situ* sputter treatment of electrodes, needs to be explored.

For implementing a plasma discharge in a working ion trapping chamber, it was successfully demonstrated that ultra-high purity (UHP) gas can be introduced into a ultra-high vacuum (UHV) system and that the pressure necessary for ion trapping experiments ($\leq \sim 10^{-10}$ Torr) can be recovered without the need to re-bake the chamber. It was also demonstrated that plasma could be localized to just above the trap chip to reduce negative effects of sputtering materials off walls, mounts and cables in the trapping chamber. Importantly the ion energies of inductively coupled plasmas (ICPs) were shown to be below the sputter threshold of the ion trap's gold and aluminum metal electrode surfaces. XPS data showed that the carbon and oxygen can be removed from both gold and aluminum surfaces for a wide range of ICP conditions, and in some instances completely for gold.

It is interesting to note that in the NIST experiments [34], a two order-of-magnitude improvement with argon ion sputtering *in situ* was observed compared to only one order-of-magnitude improvement with argon ion sputtering *ex situ*. This suggests that cleaning the trap surface of contaminants is necessary but not sufficient to attain the lowest ion heating rates.

The first step for future experiments to unequivocally understand the effects of plasma cleaning on heating rate is to remove the epoxy, used for attaching the ion trap chip to the ceramic chip carrier, given that this is a potential carbon source that can contaminate the trap surface. This will be done by using an all-metal solder die attach

method for trap, interposer, spacer, and package assembly. Pre- and post- plasma heating rate measurements for this “carbon free” trap assembly will then be performed.

Subsequent experiments should also explore how surface modifications interact with heating rates, principally argon ion beam sputtering experiments. Heating rates for samples prepared and exposed to an argon ion beam *ex situ* and followed by *in situ* plasma treatment just prior to heating rate measurements using the methods described should clarify the results to date.

In addition to the investigations described above, the cleaning of traps having electrode surfaces with distinct regions consisting of different metals should be enlightening. A shadow mask can be used to mask off different sections of the SNL trap surface to allow for two or three different metals on the same trap. It is expected that this and the above proposed studies will produce the optimal combination of surface preparation and trap electrode metal for mitigating anomalous heating. The implementation of a plasma source that can be built into a compact system that is easily integrated into existing ion trapping experiments, as demonstrated here, may be a key feature for realizing this.

## References


[1] P. W. Shor, "Polynomial-Time Algorithms for Prime Factorization and Discrete Logarithms on a Quantum Computer," *SIAM Review,* vol. 41, pp. 303-332, 1999.

[2] M. A. Nielsen and I. L. Chuang, *Quantum Computation and Quantum information*, 10th Anniversary Edition ed. Cambridge, United Kingdom: Cambridge University Press, 2010.

[3] "A Quantum Information Science and Technology Roadmap," http://qist.lanl.gov, 2004, pp. 1-11.

[4] S. Seidelin, J. Chiaverini, R. Reichle, J. J. Bollinger, D. Leibfried, J. Britton*, et al.*, "Microfabricated Surface-Electrode Ion Trap for Scalable Quantum Information Processing," *Physical Review Letters,* vol. 96, p. 253003, 06/30/ 2006.

[5] D. Kielpinski, C. Monroe, and D. J. Wineland, "Architecture for a large-scale ion-trap quantum computer," *Nature,* vol. 417, pp. 709-711, 06/13/print 2002.

[6] D. L. Moehring, C. Highstrete, D. Stick, K. M. Fortier, R. Haltli, C. Tigges*, et al.*, "Design, fabrication and experimental demonstration of junction surface ion traps," *New Journal of Physics,* vol. 13, 2011.

[7] M. Brownnutt, M. Kumph, P. Rabl, and R. Blatt, "Ion-trap measurements of electric-field noise near surfaces," 2014.

[8] Q. A. Turchette, Kielpinski, B. E. King, D. Leibfried, D. M. Meekhof, C. J. Myatt*, et al.*, "Heating of trapped ions from the quantum ground state," *Physical Review A,* vol. 61, p. 063418, 05/17/ 2000.

[9] N. Daniilidis, S. Narayanan, S. A. Moller, R. Clark, T. E. Lee, P. J. Leek*, et al.*, "Fabrication and heating rate study of microscopic surface electrode ion traps," *New Journal of Physics,* vol. 13, Jan 2011.

[10] A. I. Volokitin and B. N. J. Persson, "Adsorbate-Induced Enhancement of Electrostatic Noncontact Friction," *Physical Review Letters,* vol. 94, p. 086104, 03/03/ 2005.

[11] C. A. Dukes and R. A. Baragiola, "Compact plasma source for removal of hydrocarbons for surface analysis," *Surface and Interface Analysis,* vol. 42, pp. 40-44, 2010.

[12] J. Labaziewicz, Y. Ge, D. R. Leibrandt, S. X. Wang, R. Shewmon, and I. L. Chuang, "Temperature Dependence of Electric Field Noise above Gold Surfaces," *Physical Review Letters,* vol. 101, p. 180602, 10/30/ 2008.

[13] P. B. Antohi, D. Schuster, G. M. Akselrod, J. Labaziewicz, Y. Ge, Z. Lin*, et al.*, "Cryogenic ion trapping systems with surface-electrode traps," *Review of Scientific Instruments,* vol. 80, p. 013103, 2009.

[14] D. T. C. Allcock, L. Guidoni, T. P. Harty, C. J. Ballance, M. G. Blain, A. M. Steane*, et al.*, "Reduction of heating rate in a microfabricated ion trap by pulsed-laser cleaning," *New Journal of Physics,* vol. 13, Dec 16 2011.

[15] D. A. Hite, Y. Colombe, A. C. Wilson, K. R. Brown, U. Warring, R. Jördens*, et al.*, "100-Fold Reduction of Electric-Field Noise in an Ion Trap Cleaned with *in situ* Argon-Ion-Beam Bombardment," *Physical Review Letters,* vol. 109, p. 103001, 09/04/ 2012.

[16] I. Kazumasa, Y. Satoru, H. Kiyohiro, K. Masato, and H. Satoshi, "Sputtering yields of Au by low-energy noble gas ion bombardment," *Journal of Physics D: Applied Physics,* vol. 42, p. 135203, 2009.

[17] F. G. Major, V. N. Gheorghe, and G. Werth, *Charged Particle Traps*: Springer, 2005.

[18] B. Tabakov, F. Benito, M. Blain, C. R. Clark, S. Clark, R. A. Haltli*, et al.*, "Assembling a ring-shaped crystal in a microfabricated surface ion trap," 2015.

[19] S. X. Wang, Y. Ge, J. Labaziewicz, E. Dauler, K. Berggren, and I. L. Chuang, "Superconducting microfabricated ion traps," *Applied Physics Letters,* vol. 97, p. 244102, 2010.

[20] D. A. Gurnett and A. Bhattacharjee, *Introduction to Plasma Physics With Space and Laboratory Applications*. Cambridge, United Kingdom: Cambridge University Press, 2005.

[21] L. Tonks and I. Langmuir, "Oscillations in Ionized Gases," *Physical Review,* vol. 33, pp. 195-210, 02/01/ 1929.

[22] M. A. Lieberman and A. J. Lichtenberg, *Principles of PLasma Discharges and Materials Processing*, Second Edition ed. Hoboken, New Jersey: John Wiley & Sons, Inc., 2005.

[23] J. Hopwood, "Review of inductively coupled plasmas for plasma processing," *Plasma Sources Science and Technology,* vol. 1, p. 109, 1992.

[24] T. Okumura, "Inductively Coupled Plasma Sources and Applications," *Physics Research International,* vol. 2010, 2010.

[25] Y. Yin, J. Messier, and J. A. Hopwood, "Miniaturization of inductively coupled plasma sources," *Plasma Science, IEEE Transactions on,* vol. 27, pp. 1516-1524, 1999.

[26] M. G. Blain, J. E. Stevens, and J. R. Woodworth, "High-resolution submicron retarding field energy analyzer for low-temperature plasma analysis," *Applied Physics Letters,* vol. 75, pp. 3923-3925, 1999.

[27] M. Taborelli, "Cleaning and surface properties," in *CAS-CERN Accellerator School and ALBA Synchrotron Light Facility : Course on Vacuum in Accelerators*, ed. CERN, 2006.

[28] J. Cazaux, "The influence of radiation damage (microscopic causes) on the sensitivity of Auger electron spectroscopy and X-ray photoelectron spectroscopy," *Applications of Surface Science,* vol. 20, pp. 457-471, 2// 1985.

[29] J. Hopwood, "Planar RF induction plasma coupling efficiency," *Plasma Sources Science and Technology,* vol. 3, p. 460, 1994.

[30] D. F. McMillen and D. M. Golden, "Hydrocarbon Bond Dissociation Energies," *Annual Review of Physical Chemistry,* vol. 33, pp. 493-532
October 1982 1982.

[31] C. Ruggiero and P. Hollins, "Adsorption of carbon monoxide on the gold(332) surface," *Journal of the Chemical Society, Faraday Transactions,* vol. 92, pp. 4829-4834, 1996.

[32] F. F. Chen and J. P. Chang, *Lecture Notes on Principles of Plasma Processing*: Springer Science+Business Media, LLC, 2003.

[33] N. Daniilidis, S. Gerber, G. Bolloten, M. Ramm, A. Ransford, E. Ulin-Avila*, et al.*, "Surface noise analysis using a single-ion sensor," *Physical Review B,* vol. 89, p. 245435, 06/20/ 2014.

[34] D. A. Hite, Y. Colombe, A. C. Wilson, D. T. C. Allcock, D. Leibfried, D. J. Wineland*, et al.*, "Surface science for improved ion traps," *MRS Bulletin,* vol. 38, pp. 826-833, 2013.